1967

Hall effect of gadolinium, lutetium and yttrium single crystals

Ronald Stanley Lee
Iowa State University

HALL EFFECT OF GADOLINIUM, LUTETIUM AND YTTRIUM SINGLE CRYSTALS

by

Ronald Stanley Lee

A Dissertation Submitted to the

Graduate Faculty in Partial Fulfillment of

The Requirements for the Degree of

DOCTOR OF PHILOSOPHY

Major Subject: Experimental Physics

Approved:

Signature was redacted for privacy.

In Charge of Major Work

Signature was redacted for privacy.

Head of Major Department

Signature was redacted for privacy.

Dean of Graduate College

Iowa State University
Of Science and Technology
Ames, Iowa

1967

TABLE OF CONTENTS

I. INTRODUCTION

A. Purpose

Hall effect measurements provide information about the number and types of carriers of electrical current in a metal. In a ferromagnetic metal the Hall effect is anomalously large and exhibits a strong temperature dependence. Although there is general agreement that a spin-orbit type of interaction is responsible for the anomalous Hall effect in ferromagnetics, numerical calculations of the effect are very difficult and have met with only limited success.

Gadolinium is an interesting candidate for Hall effect measurements. It is ferromagnetic below 293°K (21). This metal has three electrons with s-d character occupying the conduction bands. The seven 4f electrons which carry the magnetic moment are shielded from direct interaction with the conduction bands by the filled 5s and 6p shells. This is in contrast to the situation with the 3d ferromagnetic transition metals where the magnetic electrons are not so localized.

Theories have been proposed that explain the qualitative features of the Hall effect in polycrystalline gadolinium (5, 9, 10, 14, 16, 28, 30). However, recent calculations (4, 11) show the Fermi surface of gadolinium to be extremely anisotropic. Measurements on single crystals are necessary to observe the effect of Fermi surface anisotropy and magnetic anisotropy on the Hall effect. The work reported here describes such measurements for the ferromagnetic metal, gadolinium, and for lutetium and yttrium.

Lutetium and yttrium are two elements which resemble gadolinium very closely in electronic structure. Lutetium differs from gadolinium only in

the occupation of the 4f shell. In lutetium the 4f shell is completely filled. Yttrium also is very similar to gadolinium. In yttrium the conduction electrons occupy overlapping 4d and 5s bands instead of 5d and 6s bands as in gadolinium. Yttrium has no partially filled shells to give a magnetic moment. Thus measurements of the Hall effect in lutetium and yttrium were undertaken in order to learn to what extent the Hall effect in gadolinium is influenced by the interaction of the conduction electrons with the polarized spins of the 4f electrons.

B. Previous Experimental Work

Hall effect measurements on polycrystalline gadolinium were first made by Kevane et al. (13). They investigated the Hall effect in polycrystalline gadolinium in the temperature range 30° - 350°C. More recent measurements by Marotta and Tauer (17), Volkenshtein and Federov (32) and Babushkina (2) have been made down to 4.2°K.

Volkenshtein et al. (33) have measured the Hall effect of two single crystals of gadolinium in the temperature range 4.2° - 370°K. They reported only values of R_1, the extraordinary Hall coefficient.

Kevane et al. (13) measured the Hall effect in polycrystalline yttrium in the temperature range 20.3° - 300°K. Anderson et al. (1) measured the Hall effect in polycrystalline lutetium in the temperature range 40° - 320°K.

Nigh et al. (21) have measured the magnetization and electrical resistivity of gadolinium single crystals. Their results have been used extensively in this investigation. The Seebeck effect in gadolinium single crystals has been measured by Sill and Legvold (27).

II. BASIC CONCEPTS AND EQUATIONS

A. Phenomenological Theory

If a magnetic field intensity, $\vec{H}$, is applied to a conductor which carries a current density, $\vec{J}$, an electric field, $\vec{E}_H$, is set up in a direction perpendicular to $\vec{H}$ and $\vec{J}$. This effect is called the Hall effect. $\vec{E}_H$ is called the Hall electric field and is related to the current density and magnetic field, $\vec{B}$, by

$$\vec{E}_H = -R_o (\vec{J}X\vec{B}) \tag{2.1}$$

where R_o is called the ordinary Hall coefficient. If appreciable magnetization exists in the sample, the Hall effect may be described by

$$\vec{E}_H = -R_o (\vec{J}X\vec{H}) - R_1 (\vec{J}X\vec{M}) \tag{2.2}$$

where $\vec{M}$ is the magnetization and R_1 is called the extraordinary Hall coefficient. Typically, R_1 is one or two orders of magnitude larger than R_o.

If the Hall effect is measured in anisotropic single crystals, the observed Hall coefficient will depend on the orientation of the crystal with respect to $\vec{J}$ and $\vec{H}$. To understand this orientation dependence one must consider the dependence of the resistivity tensor on the magnetic field intensity, $\vec{H}$, and the magnetization, $\vec{M}$. One must consider $\vec{M}$ and $\vec{H}$ as independent variables because the part of the Hall effect that depends on $\vec{M}$ does not arise from that part of the magnetic induction, $\vec{B}$, due to $\vec{M}$ but is rather due to a spin-orbit interaction which is dependent on $\vec{M}$. If one expands the resistivity tensor as a power series in $\vec{M}$ and $\vec{H}$, one

obtains to first order in $\vec{M}$, $\vec{H}$

$$\rho_{ij}(M,H) = \rho_{ij}(0) + \rho_{ijk}H_k + \rho'_{ijk}M_k + \ldots \quad . \tag{2.3}$$

The electric field inside a sample carrying current density $\vec{J}$ in a magnetic field intensity $\vec{H}$ is then

$$E_i = \rho_{ij}(0)J_j + \rho_{ijk}J_jH_k + \rho'_{ijk}J_jM_k \tag{2.4}$$

to first order in $\vec{M}$, $\vec{H}$ where in both Equations 2.3 and 2.4 we sum over repeated indices.

Equation 2.4 may be simplified in several ways. From Equation 2.1 we see that the Hall electric field is defined to be that component of the electric field perpendicular to both current and magnetic field directions. This eliminates all ρ_{ijk} for which $i = j$, $i = k$ or $j = k$ from our consideration, although such terms need not necessarily vanish. Further we may apply Onsager's theorem as stated in (34). This theorem states that $L_{ij}(\vec{H}) = L_{ji}(-\vec{H})$ where the L_{ij} are coefficients relating generalized forces and currents and are defined to make the entropy production a quadratic form in the thermodynamic forces. With these simplifications our resistivity tensor may be written

$$[\rho_{ij}] = \begin{bmatrix} (\rho_{11}) & (\rho_{12}-\rho_{213}H_3-\rho'_{213}M_3) & (\rho_{13}+\rho_{132}H_2+\rho'_{123}M_2) \\ (\rho_{12}+\rho_{213}H_3+\rho'_{213}M_3) & (\rho_{22}) & (\rho_{23}-\rho_{321}H_1-\rho'_{321}M_1) \\ (\rho_{13}-\rho_{132}H_2-\rho'_{132}M_2) & (\rho_{23}+\rho_{321}H_1+\rho'_{321}M_1) & (\rho_{33}) \end{bmatrix} \tag{2.5}$$

where we have assumed that $\vec{M}$ and $\vec{H}$ are in the same direction.

From Equations 2.4 and 2.5 we see that the Hall effect is characterized

by the direction in which the magnetic field intensity, $\vec{H}$, is applied. Interchanging the direction of current flow and the direction in which the Hall voltage is measured gives the same Hall coefficients. If the crystal in which the Hall effect is measured has hexagonal symmetry there are only two independent Hall coefficients, one for $\vec{H}$ applied along the c-axis and one for $\vec{H}$ along an a-axis or b-axis. This may be demonstrated by transforming the resistivity tensor to a coordinate system rotated 60^{o} about the c-axis and rotating the direction of $\vec{H}$ by the same transformation. The sixfold symmetry of the hexagonal lattice requires that the same fields be observed in the transformed system, which yields the desired result.

It is also of interest to relate the two Hall coefficients observed in single crystal samples of hexagonal symmetry to the Hall coefficient measured in a polycrystalline sample of the same material.

Consider a single crystal sample whose crystalline axes have an arbitrary orientation with respect to a fixed set of axes defined by $\vec{H}$, $\vec{J}$ and $\vec{J}X\vec{H}$. If we describe the orientation of the crystalline axes with respect to the fixed axes by the Euler angles, θ, Φ, and Ψ, and if we let $\vec{H} = (0,0,H)$, $\vec{J} = (J,0,0)$, then E_H is given by

$$E_H/J = [R_o(\perp)\sin^2\theta + R_o(\parallel)\cos^2\theta]H + [R_1(\perp)\sin^2\theta + R_1(\parallel)\cos^2\theta]M + G(\theta,\Phi,\Psi) \qquad (2.6)$$

Where $R_o(\parallel)$ and $R_o(\perp)$ are the ordinary Hall coefficients of a hexagonal crystal measured with $\vec{H}$ applied parallel and perpendicular to the axis of symmetry and similarly for $R_1(\parallel)$ and $R_1(\perp)$. $G(\theta,\Phi,\Psi)$ is a function which vanishes when averaged over the total solid angle. An average over the

total solid angle gives the Hall effect for a polycrystalline sample,

$$R_o(\text{poly.}) = 1/3\ R_o(\parallel) + 2/3\ R_o(\perp)$$

$$R_1(\text{poly.}) = 1/3\ R_1(\parallel) + 2/3\ R_1(\perp) \quad . \tag{2.7}$$

B. The Hall Effect in Non-magnetic Metals

The origin of the Hall effect can be most simply understood by considering the forces acting on a charge carrier moving in a conductor carrying current density, $\vec{J}$, with a magnetic field intensity, $\vec{H}$, applied perpendicular to $\vec{J}$. In the steady state the net transverse force on the charge carriers must be zero. This condition may be expressed as

$$\vec{F}_{tr} = 0 = q(\vec{E}_H + \vec{J}X\vec{B}/nqc) \tag{2.8}$$

giving the simple result

$$\vec{E}_H = -R_o\ \vec{J}X\vec{B} \tag{2.9}$$

where

$$R_o = 1/nqc \quad . \tag{2.10}$$

In the Equations 2.8, 2.9 and 2.10, n is the number of charge carriers per unit volume, q is the charge of an individual carrier, c is the velocity of light and the cgs system of units is used. R_o is called the ordinary Hall coefficient and is defined positive for holes and negative for electrons. Equation 2.10 is well obeyed for metals whose electrons are nearly free, but a more careful treatment is required when two or more bands are involved or when the Fermi surface is non-spherical.

It can be shown (22) that for a metal having two Fermi surfaces, each spherical, one containing n_- electrons, the other containing n_+ holes, the Hall coefficient at low fields is given by

$$R_o \simeq (1/ec)(n_- - n_+)/(n_- + n_+)^2 \qquad (2.11)$$

where e is the charge of the electron.

For a metal with P spherical Fermi surfaces of either electrons or holes, the arguments used to derive Equation 2.11 yield the result

$$R_o \simeq (e/\sigma^2 c) \sum_{j=1}^{P} n_j \mu_j^2 \qquad (2.12)$$

where σ is the total conductivity, μ_j is the conductivity mobility of the jth surface and n_j is the number of carriers in the jth surface. n_j is defined negative for holes and positive for electrons.

In the case of the rare earth metals, however, the Fermi surfaces are decidedly non-spherical (4, 11, 15). The expressions given above for the Hall coefficient are valid for the rare earths only in the sense that they might give an indication of the possible mechanisms by which the observed results may be explained.

Jones and Zener (7) have proposed a method by which the Hall coefficient may be calculated for an arbitrary Fermi surface, but in practice the integrals involved are extremely formidable. Since Fermi surface calculations have been made only recently on rare earth metals, no such calculations exist for them at this writing.

C. The Hall Effect in Ferromagnets

In a ferromagnetic metal the Hall effect may be described by the equation

$$e_H = R_o H + R_1 M \tag{2.13}$$

where H is the magnetic field intensity inside the sample, M is the magnetization and e_H is the Hall electric field per unit current density.

The behavior of R_1, the extraordinary Hall coefficient, cannot be accounted for on the basis of a simple Lorentz force picture. There seems to be general agreement among existing theories that the anomalous behavior of the Hall effect in ferromagnetics is due to a spin-orbit interaction (5, 9, 10, 14, 16, 28, 30).

The first successful treatment of the ferromagnetic Hall effect was given by Karplus and Luttinger (10). They investigated the intrinsic spin-orbit interaction of polarized electrons. Their calculations predicted that R_1 should be proportional to the square of the resistivity. Other investigations have been made by Luttinger (10), Smit (28), Strachan and Murray (30), Gurevich and Yassievich (5), Kagan and Maksimov (9) and Leribaux (14). The only attempts to calculate R_1 numerically were made by Strachan and Murray for Ni (30) and by Leribaux for Fe (14).

It has been pointed out (30) that the ρ^2 dependence of the ferromagnetic Hall coefficient, R_1, is simply the result of inverting the conductivity tensor. If x is the direction of current flow, z the direction of the magnetization and y the direction of the Hall field, we have the relation

$$J_i = \Sigma \sigma_{ij} E_j \quad . \tag{2.14}$$

With $J_y = 0$ we obtain for the Hall resistivity

$$e_H = E_y/J_x = -\sigma_{yx}/\sigma_{xx}\sigma_{yy} \tag{2.15}$$

under the condition $(\sigma_{yx})^2 \ll \sigma_{xx}\sigma_{yy}$ which is well obeyed experimentally. This ρ^2 dependence is quite a general result. Since σ_{yx} depends only on the spin system and not on the scattering, the temperature dependence will come mainly from the $\sigma_{xx}\sigma_{yy}$ term in the denominator of Equation 2.15 unless the magnetization or Fermi surface is strongly temperature dependent.

III. EXPERIMENTAL PROCEDURE

A. Measurement of the Hall Effect - d.c. Method

If a sample of thickness, t, carrying current, I, is placed in a magnetic field intensity, H, a Hall voltage, V_H, will be developed across the sample as shown in Figure 1. V_H is related to e_H, the Hall electric field per unit current density, by

$$e_H = V_H t/I \quad . \tag{3.1}$$

A study of the Hall effect thus involves measuring V_H, t, I, H and T, the sample temperature.

V_H, the Hall voltage, was measured with a Honeywell model 2768 six dial potentiometer, Guildline Type 5214/9460 photocell galvanometer amplifier and a Guildline Type SR21/9461 secondary galvanometer. These instruments provided a voltage resolution of 0.01 microvolts.

A drawing of the sample holder is shown in Figure 2. The sample was clamped in place between phosphor-bronze strips at the ends of the sample. These strips also served as current contacts. The Hall voltage probes were 0.020 inch diameter tungsten wires on which a knife edge had been ground. These were clamped on the underside of the sample holder and protruded through the sample holder on either side of the sample. The wire was springy enough to provide good electrical contact down to liquid helium temperatures. All electrical connections in the Hall voltage measuring circuit were copper-to-copper with the exception of the copper-to-tungsten and tungsten-to-sample connections in the sample holder.

Ideally, the Hall probes should be aligned exactly opposite one

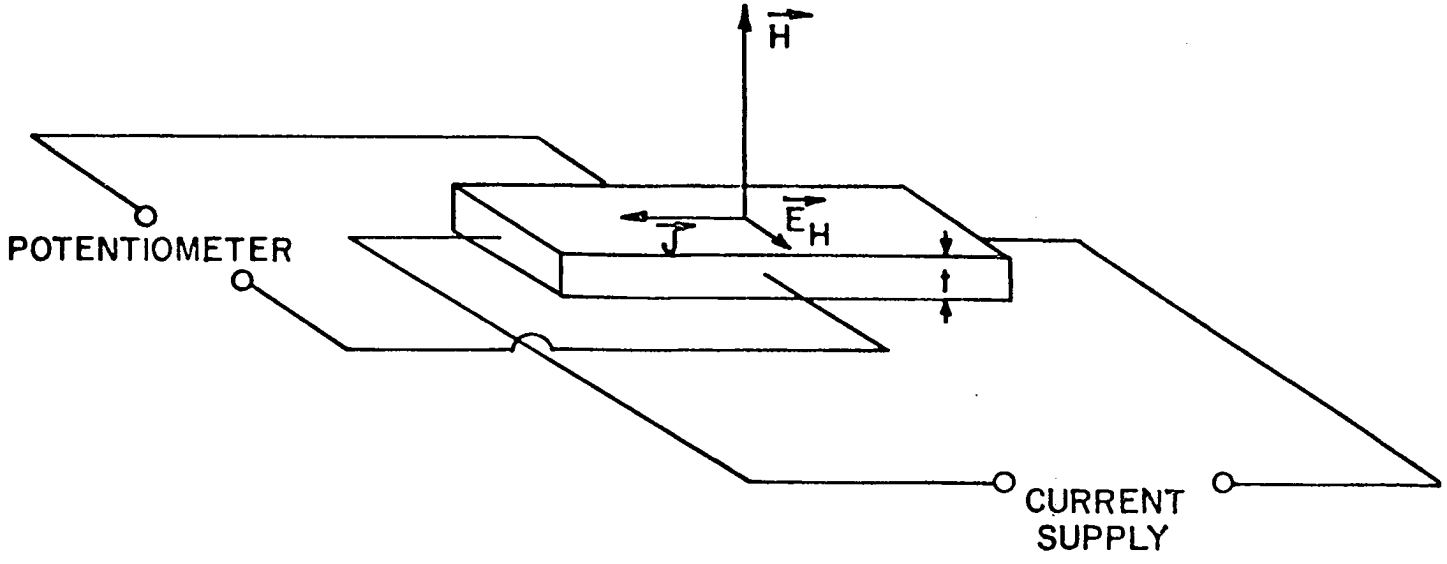

Figure 1. A schematic drawing of the relation between $\vec{J}$, $\vec{H}$ and $\vec{E}_H$ and of the measuring circuit

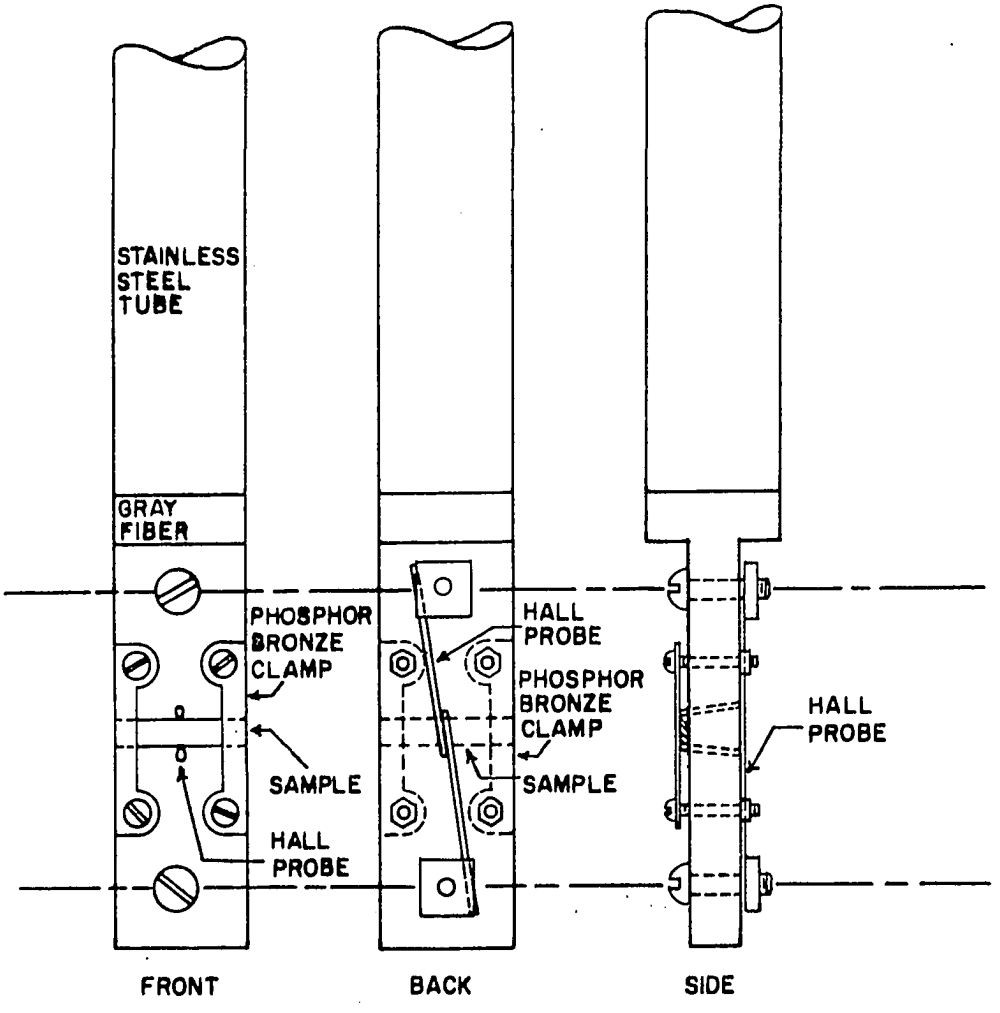

Figure 2. Drawing of the sample holder

another so they touch the sample on the same equipotential line. In practice this is not achieved. Because of the high resistivity of the rare earth metals, a slight misalignment of the probes produced an appreciable zero field voltage. One cannot simply subtract this voltage from the voltage measured with an applied field because the voltage due to probe misalignment changes with H due to magnetoresistance.

One must also take into account the thermal emfs produced at the various junctions in the measuring circuit.

These thermal and resistive voltages were separated from the true Hall voltage by means of current and magnetic field reversal. The zero field voltage was first measured for forward and reverse current. The average of these two voltages is the true zero field voltage because the thermal emfs do not reverse with current. The magnetic field was then increased in steps up to the maximum value, the forward and reverse voltage being measured at each step. When the maximum field was reached, the sample was demagnetized by rotating the sample back and forth as the field was turned back down to zero. This process was then repeated with the magnetic field in the opposite direction. Field reversal was achieved by rotating the sample 180^{o} from its original position. By averaging the results for forward and reverse fields the magnetoresistance effects are eliminated, since $\Delta\rho$ is an even function of B, the magnetic induction. The true Hall voltage, $V_H(H)$, is calculated from the equation

$$V_H(H) = 1/4([V_+(H)-V_-(H)] + [V_+(-H)-V_-(-H)] - 2[V_+(0)-V_-(0)]) \quad . \qquad (3.2)$$

This equation is merely a statement of the averaging procedures described above. $V_+(H)$ is the Hall voltage with the current forward and the

magnetic field in the forward direction. $V_-(-H)$ is the Hall voltage with current and field reversed and similarly for $V_-(H)$ and $V_+(-H)$. $V_\pm(0)$ is the zero field voltage.

The sample thickness, t, was measured with a Steinmeyer 25-50 mm. metric micrometer and a 25 mm. gauge block. This instrument measured to within 0.001 mm.

The sample current, I, was determined by measuring the voltage across a 0.01 ohm standard resistor which was connected in series with the sample. This voltage was measured with a Rubicon Type K2 potentiometer and a Leeds and Northrop galvanometer. The current supply was constructed in the electronics shop at the Ames Laboratory and was regulated to 0.01% Sample currents were about 0.125 amperes. Larger currents than this heated the sample and resulted in excessive thermal emfs.

The magnetic field was produced by a Harvey-Wells L-158 electromagnet and HS-200 kw. power supply. This magnet produced a maximum field of 30.7 kOe. Field calibration was made with a Rawson Type 501, 0.1%, rotating coil gaussmeter.

Alignment of the sample perpendicular to the magnetic field was made by means of a rotating sample holder assembly as described by Rhyne (25). This device allowed the sample to be rotated in the magnetic field by remote control. The sample was put into the cryostat with the approximate orientation for the forward magnetic field direction. The rotating sample holder assembly was set to 0^o and the magnet was rotated about the vertical axis to give a maximum Hall voltage. The 0^o setting then gave the forward field and the 180^o setting gave the reverse field. The variation of the Hall voltage with angle was symmetrical about 0^o and 180^o when the

sample was aligned in this way.

The sample temperature, T, was measured by thermocouples mounted directly beneath the sample. A Cu versus constantan thermocouple was used about 20°K and a Au-Fe versus Cu thermocouple was used below 20°K. The calibration used for the constantan wire was that reported by Powell et al. (23). Two different Au-Fe versus Cu thermocouples were used because one of the thermocouples broke during the course of the experiment. The composition of the first was Au 0.07 at.% Fe and the calibration on this wire was performed by Finnemore et al. (3). The thermocouple which replaced it had composition Au 0.03 at .% Fe. This roll of wire was calibrated by W. Gray of this laboratory by comparison with a calibrated germanium resistor.

Individual thermocouples prepared from the same roll of thermocouple wire differ by several microvolts at low temperatures, presumably due to inhomogeneous distribution of impurities in the wire. The thermocouples used in this experiment were normalized to the calibration curves by the method described by Rhyne (25). Thermocouple junctions were made with soft solder. Thermocouple voltages were measured with a Rubicon Type K2 potentiometer and a Honeywell galvanometer. All thermocouple leads and all leads coming to the sample were thermally anchored by wrapping the leads several times around the bottom of the stainless steel sample tube and cementing them to the tube with General Electric 7031 varnish. The absolute accuracy of the temperature measurements is estimated to be $\pm$ 0.5°K and the relative accuracy is about 0.1°K over the range 4.2°K to 350°K.

The temperature of the sample was controlled to $\pm$ 0.1°K by means of a

temperature control amplifier and bridge as described in (20, 25, 27). A nitrogen shielded dewar was used for these measurements. This was the same dewar used by Rhyne and is described in (25). Measurements were made over the temperature range $4.2^{o}K$ to $340^{o}K$.

B. Measurement of the Hall Effect - a.c. Method

Hall effect measurements for the lutetium and yttrium samples were made on an a.c. Hall effect apparatus. This apparatus was designed and constructed by L. D. Muhlestein and is described in detail in his Ph.D. dissertation (18). It was necessary to resort to using an a.c. technique on the lutetium and yttrium samples because the Hall effect in these metals was too small for the d.c. apparatus.

Figure 3 shows a block diagram of the a.c. Hall apparatus. A 386 cycle per second signal was produced by a Hewlett-Packard Model 203A signal generator. This signal was amplified by a Hewlett-Packard Model 467A power amplifier to supply the a.c. current to the sample. The current was determined from a measurement of the voltage drop across a 0.1 ohm standard resistor with a Fluke Model 883AB differential voltmeter.

The a.c. signal from the signal generator was also used as the reference signal for a Princeton Applied Research Model JB-5 phase sensitive lock-in amplifier as well as for two bucking circuits. The first bucking circuit was used to buckout the zero field voltage due to misalignment of the Hall probes. The second bucking circuit contained a phase shifter followed by a Fluke Model 883 AB differential voltmeter and a Dekatran Model DT72A decade transformer. The second bucking circuit measured the unknown signal from the Hall probes or the resistivity probes

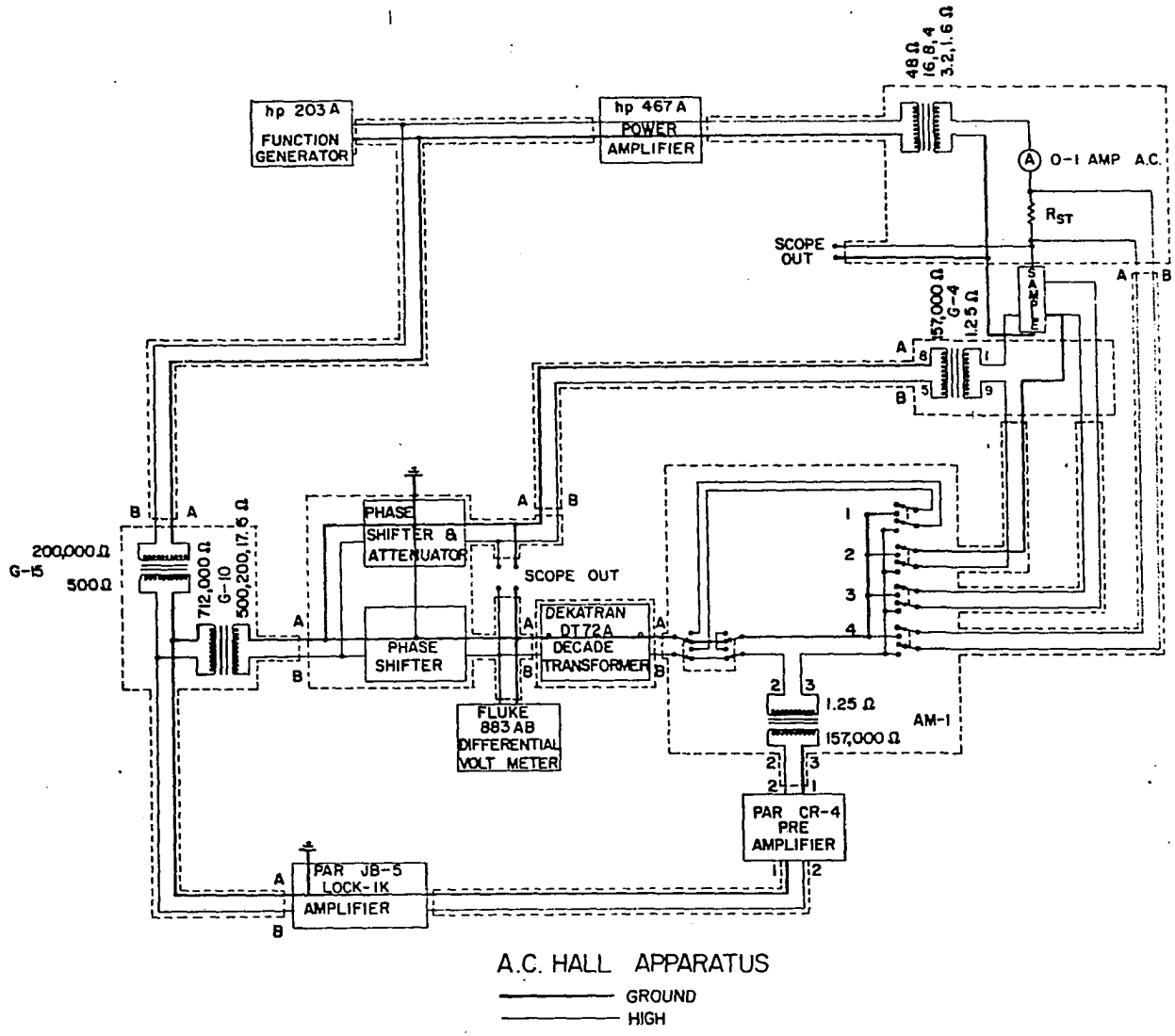

Figure 3. Block diagram of the a.c. Hall effect apparatus

by providing a signal 180 degrees out of phase with the unknown signal and of equal magnitude. The null was detected by a Princeton Applied Research Model CR-4 pre-amplifier and a Model JB-5 lock-in amplifier. This apparatus provided a voltage resolution of 10^{-9}volt.

The Hall voltage was measured at the maximum field and the Hall coefficient was computed from the equation

$$R_o = V_H \, t/IH \quad . \tag{3.3}$$

It was not practical to measure the Hall voltage as a function of H because of the extremely small signals. The linearity of V_H with H was checked on the yttrium c-axis sample and V_H was found to be linear with H within the limits of error.

The sample holder of the a.c. apparatus is described in detail in (18). This sample holder differs somewhat in design but is equivalent in operation to the sample holder used for the d.c. measurements.

Temperatures were measured with a copper versus constantan and a copper versus Au 0.07% Fe thermocouple.

The magnet used for the a.c. measurements was a six inch Varian with a Varian V2100B power supply. This system provided magnetic fields up to 7.8 kOe. The magnetic field was measured with a Radio Frequency Laboratories Model 1890 gaussmeter. This gaussmeter was calibrated against a 0.1% Rawson Type 501 rotating coil gaussmeter.

All of the determinations of R_o were averaged over forward and reverse field directions. The resistivity ratio was measured for all of the samples.

C. Sample Preparation

As was mentioned earlier, it is necessary to study single crystal specimens to observe the effects of Fermi surface anisotropy and magnetic anisotropy on the Hall effect.

The rare earth metals used in this investigation were produced at the Ames Laboratory by use of an ion exchange process for the separation of the rare earth compounds (29) and a reduction process for the preparation of the pure metal from the fluoride.

The single crystals from which the samples were cut were grown from arc-melted buttons of pure metal by a thermal-strain-anneal technique described by Nigh (19). Thermal strains which were frozen into the button by the arc-melting process were removed by annealing the metal button at a temperature slightly below the melting point. The gadolinium crystals used in this investigation were those from which Sill (27) had obtained his samples. The lutetium and yttrium crystals were grown by the author.

The crystals grown by this technique were aligned by Laue back-reflection of x-rays. The samples were cut to approximate dimensions by a Servomet spark-erosion apparatus. The samples were then hand lapped to final dimensions with carborundum paper and were finally etched or electropolished to ensure a surface to which good electrical contact could be made.

The samples were cut in the form of a rectangular parallelepiped. The gadolinium samples had dimensions of approximately 1 cm. x 2.5 mm. x 0.5 mm. The lutetium and yttrium samples were somewhat smaller so they would fit into the a.c. Hall effect apparatus sample holder. The ratio of length to width of all of the samples was at least 4:1 to eliminate shorting effects

(6).

The thinness of the samples was necessary to produce a larger V_H, but the thin samples also require a relatively large correction for demagnetizing fields. The demagnetization factor for each sample was calculated by the method of Joseph and Schlömann (8). Sample dimensions and demagnetization factors are listed in the Appendix.

The rare earth metals used in this investigation were of the best purity available at the Ames Laboratory. Scraps of metal left over after the samples were cut were heavily etched to remove surface impurities and were analyzed for impurities by a semi-quantitative spectrographic analysis and a quantitative vacuum fusion analysis for dissolved gas impurities. These analyses were made at the Laboratory. Resistivity ratios, $\rho_{300^oK}/\rho_{4.2^oK}$, were measured for all the samples. Information regarding sample purity is tabulated in the Appendix.

D. Determination of R_o and R_1 from Isothermal Data

In this investigation the Hall effect was measured isothermally, i.e., the temperature was held constant and the variation of the Hall voltage with magnetic field was measured. If the sample is paramagnetic the ordinary Hall coefficient is given by Equation 3.3 and is independent of H.

If the sample is ferromagnetic, a more complex procedure is necessary to extract the coefficients R_o and R_1 from the isothermal data. For a ferromagnetic material we must use the equation

$$e_H = R_o H + R_1 M \quad . \tag{3.4}$$

It is convenient to write this in terms of the applied field, $H_{app.}$, as

$$e_H = R_o H_{app.} + (R_1 - NR_o)M \tag{3.5}$$

where we assume we can write

$$H = H_{app.} - NM \quad . \tag{3.6}$$

N is called the demagnetizing factor and is, in reality, a complicated tensor quantity. Equation 3.6 holds only to first order for non-ellipsoidal samples. Joseph and Schlömann (8) have calculated N as a power series in ascending powers of M/H. Their result has been assumed to be good to a first approximation above magnetic saturation where M/H will be small. Since N also varies with position inside the sample, the value of N used for each sample represents an average over the sample. Figure 4 shows the variation of N_{zz} in various directions from the center of a sample with dimensions 1 cm. x 2.5 mm. x 0.4 mm.

Above saturation M/H = 0 so R_o is given by

$$R_o = (\partial e_H/\partial H)_{H > H_s} \tag{3.7}$$

where H_s is the applied field necessary to saturate the sample and H is now taken to be the applied field.

We can determine R_1 also, for

$$e_H\big|_{H > H_s} = R_o H + (R_1 - NR_o)M_s \tag{3.8}$$

where M_s is $M(H = \infty)$, the saturation magnetization. Values of M_s for gadolinium were obtained from the data of Nigh (20). Equation 3.8 is

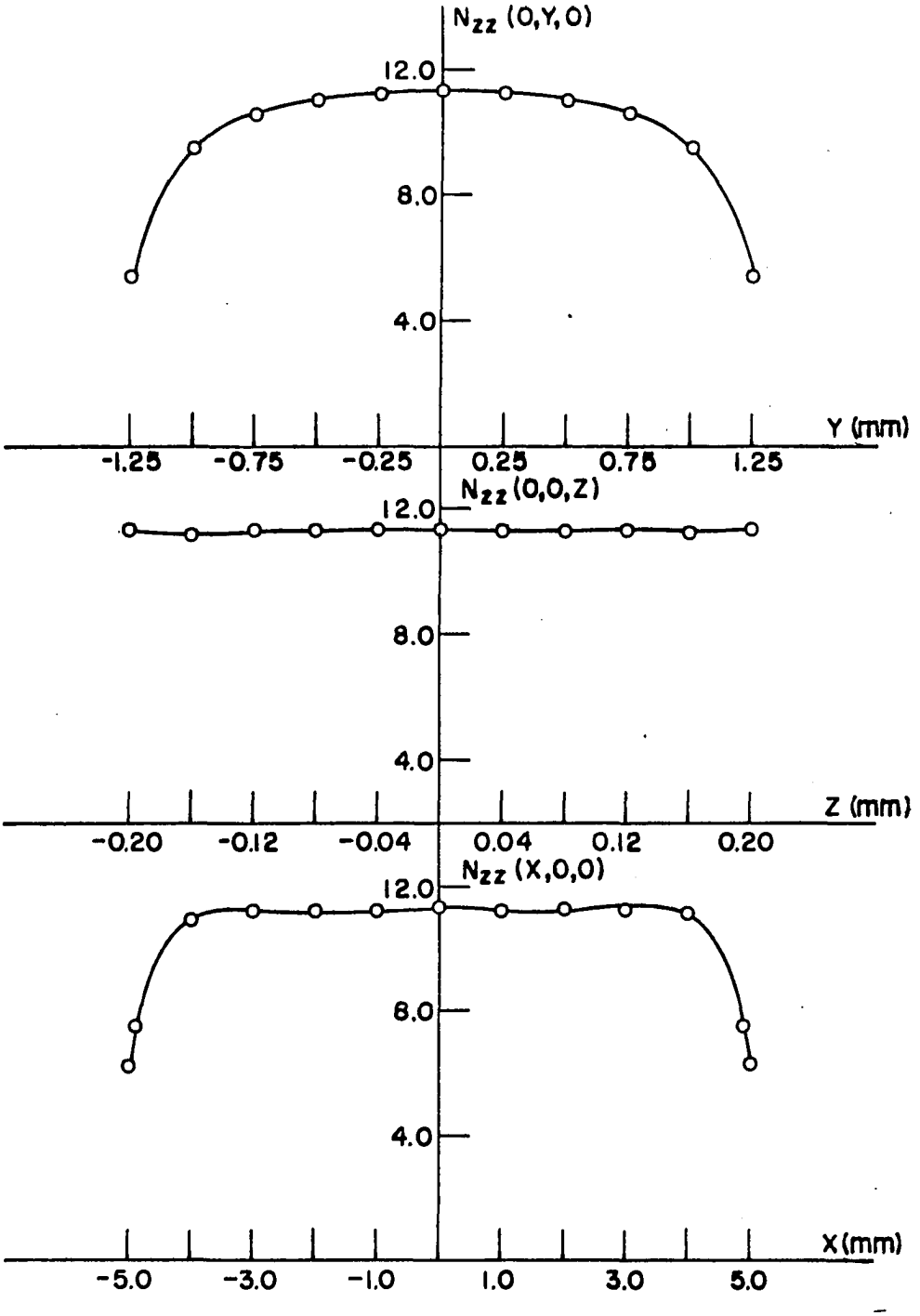

Figure 4. The variation of N_{zz} in various directions from the center of a sample with dimensions 1 cm. x 2.5 mm. x 0.4 mm.

linear and if it is extrapolated to H = 0 one obtains the result

$$\mathfrak{A} = (R_1 - NR_o)M_s \tag{3.9}$$

where $\mathfrak{A}$ is the intercept of the linear portion of the e_H versus H curve on the e_H axis. From this we have

$$R_1 = (\mathfrak{A} + NR_oM_s)/M_s \quad . \tag{3.10}$$

A correction to Equation 3.7 must be made to take into account the high field susceptibility, χ_s, of the sample above saturation. Because of the small linear dependence of M on H above saturation, we must include a term depending on R_1 in the expression for R_o. We then have

$$\partial e_H/\partial H\big|_{H > H_s} = R_o + R_1\chi_s \quad . \tag{3.11}$$

Since the term depending on R_o in Equation 3.10 is small compared to R_1 in ferromagnetic materials, we may substitute $\partial e_H/\partial H\big|_{H > H_s}$ for R_o in this equation with little error. The value of R_1 thus computed may then be used in Equation 3.11 to determine R_o. In gadolinium $R_1\chi_s$ is as large as 30% of R_o near the ferromagnetic Curie temperature, θ_c, so this is an important correction. χ_s for gadolinium was determined from the magnetization data of Nigh by computing the slope of the M versus H curves above saturation. χ_s for gadolinium is shown as a function of temperature in Figure 5.

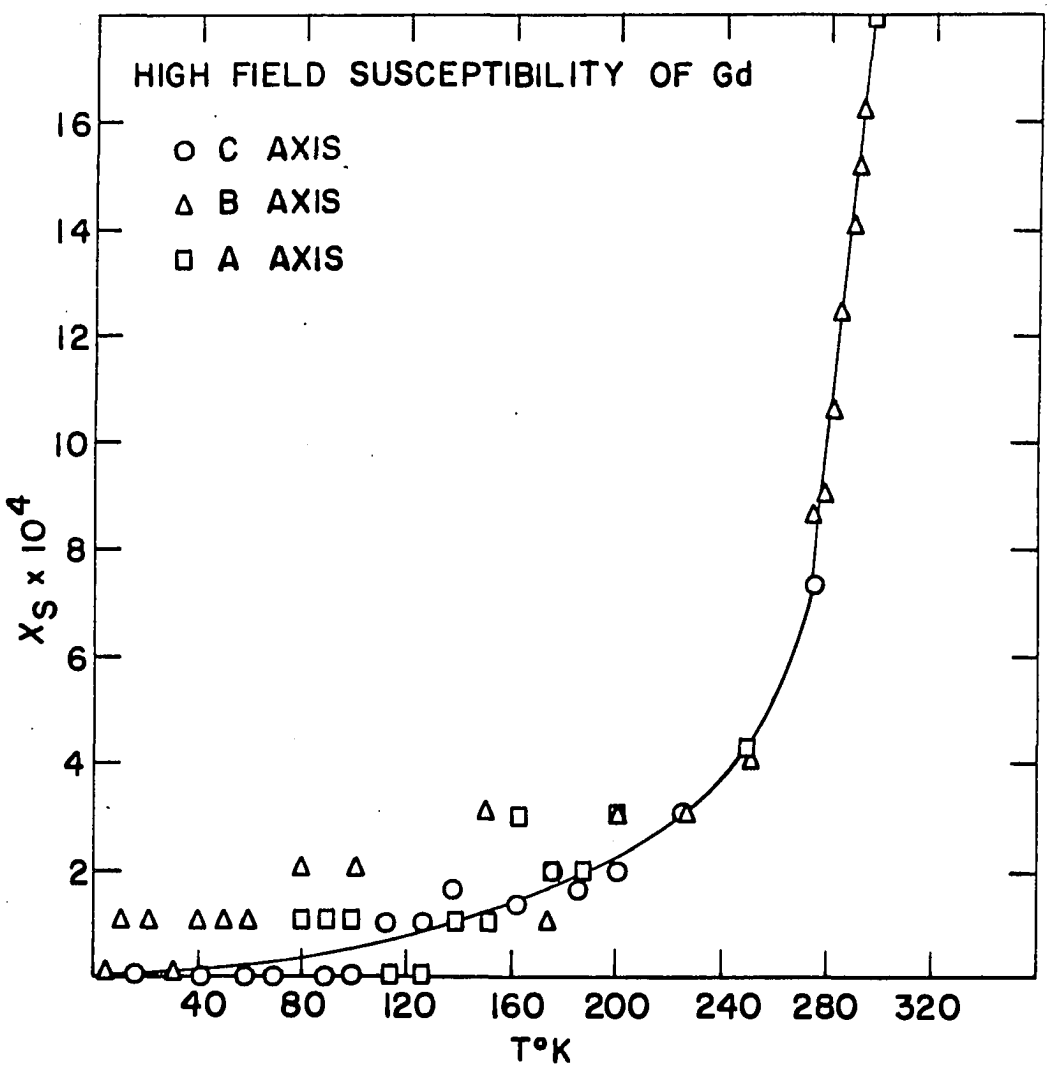

Figure 5. χ_s for gadolinium single crystals as a function of temperature

IV. EXPERIMENTAL RESULTS

A. Gadolinium

The Hall voltage, V_H, was measured for four single crystals of gadolinium over the temperature range 4.2° to 340°K in magnetic fields up to 30.7 kOe. The orientations of the four crystals are listed in Table 1.

Table 1. Orientations of gadolinium single crystal samples.

Sample	H	J	e_H	Designation
Gd I	b-axis	c-axis	a-axis	b-axis
Gd II	a-axis	c-axis	b-axis	a-axis
Gd III	a-axis	b-axis	c-axis	a-axis
Gd IV	c-axis	b-axis	a-axis	c-axis

The data were taken isothermally, that is, the Hall voltage was measured as a function of applied magnetic field while the sample temperature was held constant. For each temperature the magnetic field was varied from 0 to 30.7 kOe. Figure 6 shows representative isotherms for the c-axis sample. Figure 7 shows representative isotherms for an a-axis sample. One can see from the linear portions of these curves at high fields that the samples are magnetically saturated in spite of the large demagnetizing fields. All of the isothermal data are tabulated in the Appendix. Figure 8 is a plot of e_H versus T for H = 30.7 kOe. Data for all of the samples are plotted on the same graph. A large anisotropy is observed between the c-axis sample and the a and b-axis samples which will from now on be called the basal plane samples. No basal plane anisotropy is observed. This presentation of the data is useful to show the size of the Hall effect as a function of temperature.

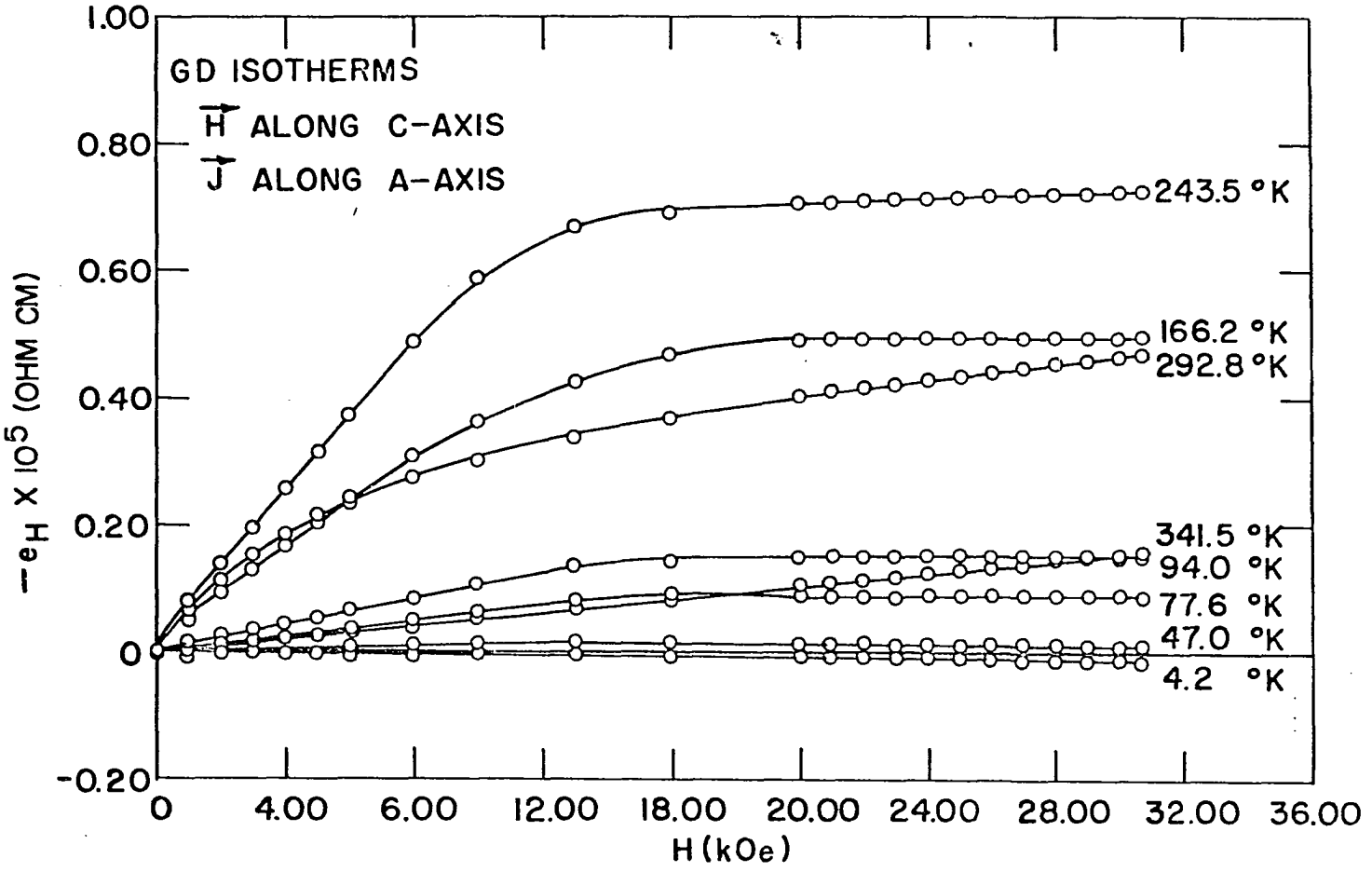

Figure 6. Isotherms for the gadolinium c-axis sample

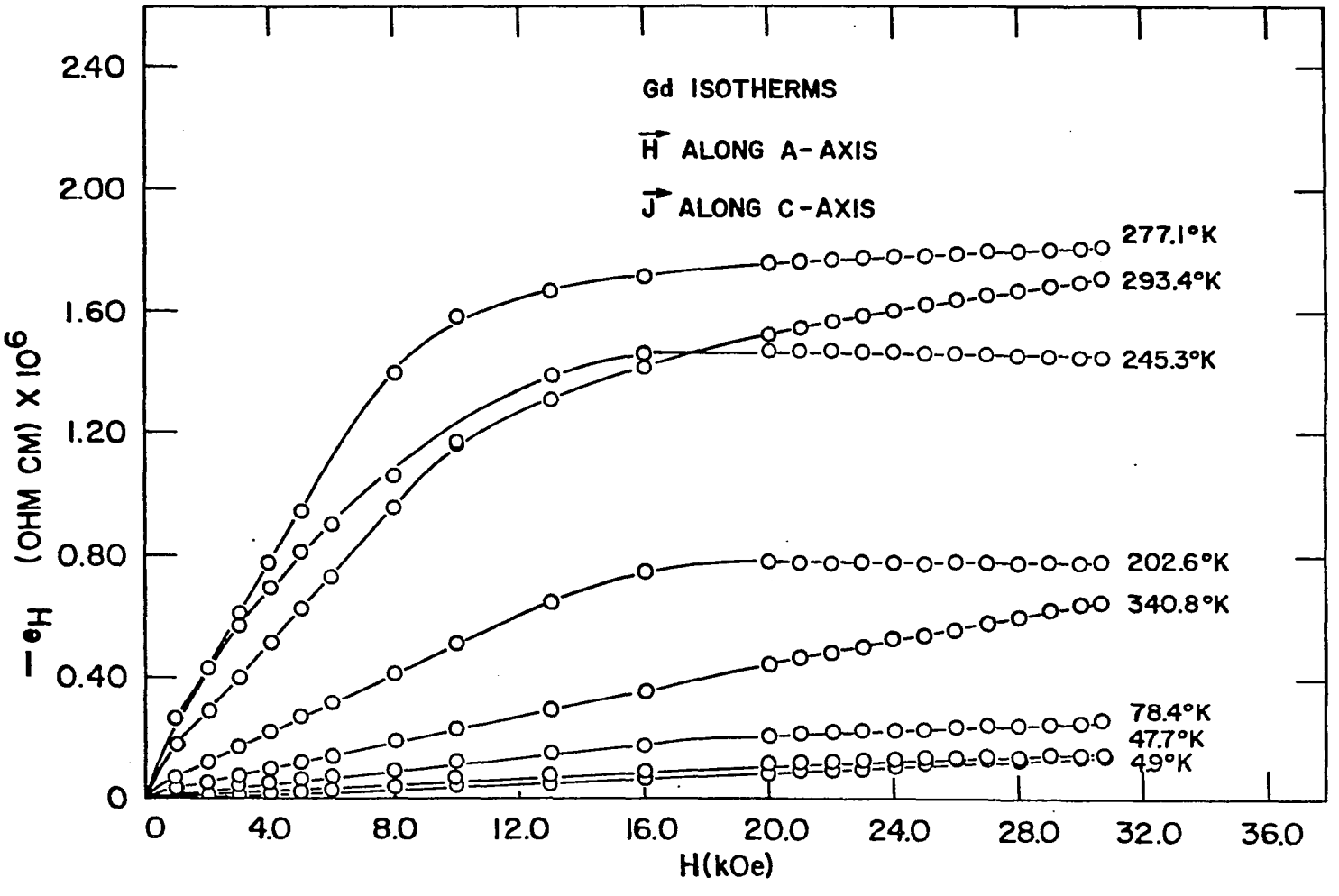

Figure 7. Isotherms for a gadolinium a-axis sample

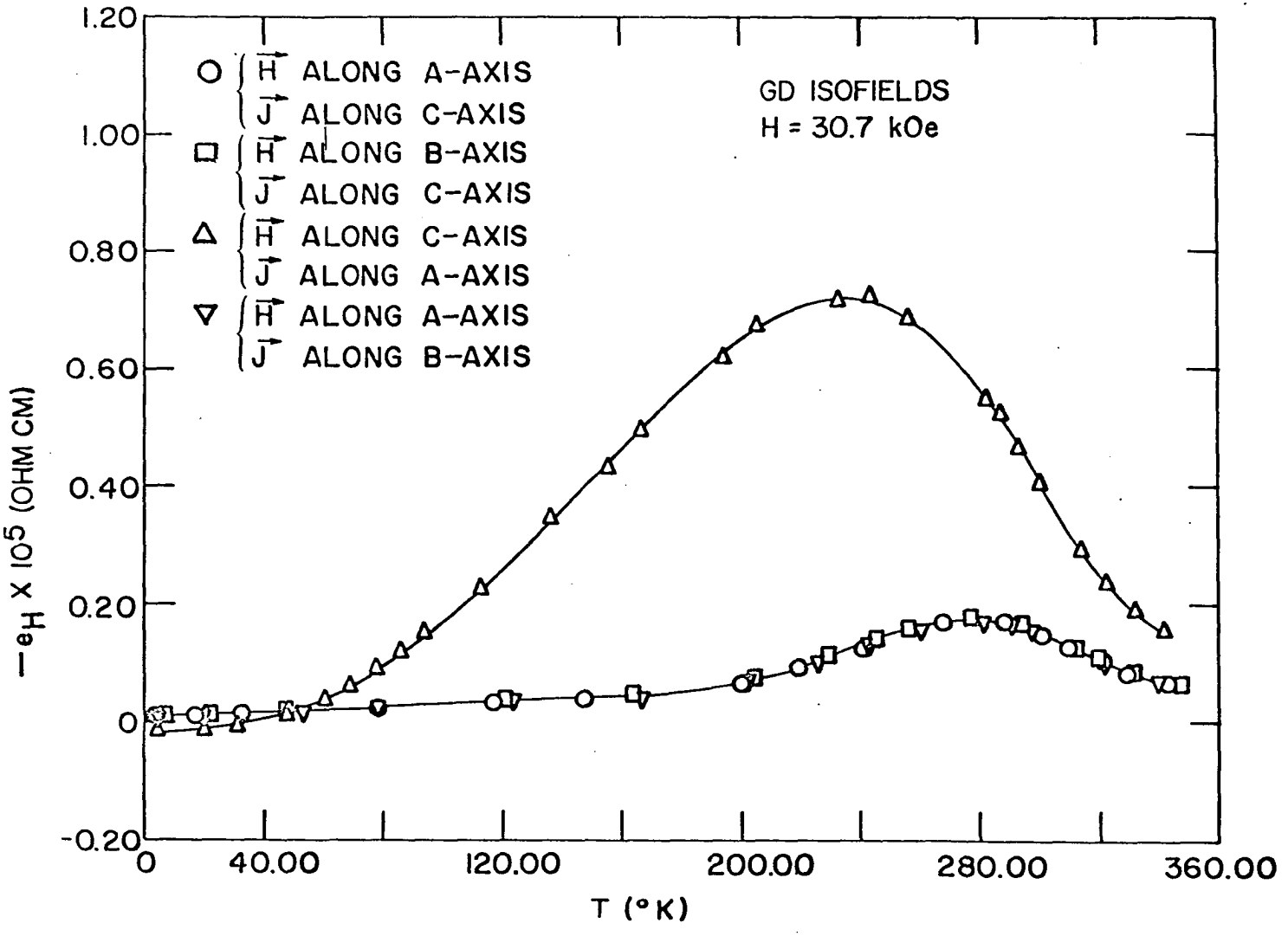

Figure 8. e_H versus T for H = 30.7 kOe. Data from all of the samples are plotted on the same graph

R_o, the ordinary Hall coefficient, is plotted as a function of temperature in Figure 9. A large anisotropy between the c-axis and basal plane samples is observed but no basal plane anisotropy can be observed. Since the data for Gd II and Gd III are the same, within the limits of error, it can be seen that the direction of J in the crystal does not affect the value of R_o. This is in agreement with the prediction of the phenomenological theory that the direction of H and M determined which component of the resistivity tensor would be measured.

Interesting features of these curves are the sharp rise in R_o near θ_c and the changes in sign of R_o at 195°K and 277°K for the basal plane samples and at 130°K for the c-axis sample.

Figure 10 shows R_1, the extraordinary Hall coefficient, plotted as a function of temperature. Again one observes a large anisotropy between the c-axis and basal plane samples and no basal plane anisotropy. R_1 does not have its maximum value at θ_c, but rather at about 280°K for the basal plane samples and about 250°K for the c-axis sample.

Figure 11 shows the values of R_1 for single crystals of gadolinium as measured by Volkenshtein et al. (33) compared to the findings of the present investigation. The agreement is relatively good for the c-axis sample but is not so good for the basal plane samples. Volkenshtein et al. (33) report no values for R_o.

R_o and R_1 have been determined only up to 293°K because above the Curie temperature it is not possible to separate the effects due to R_o and R_1.

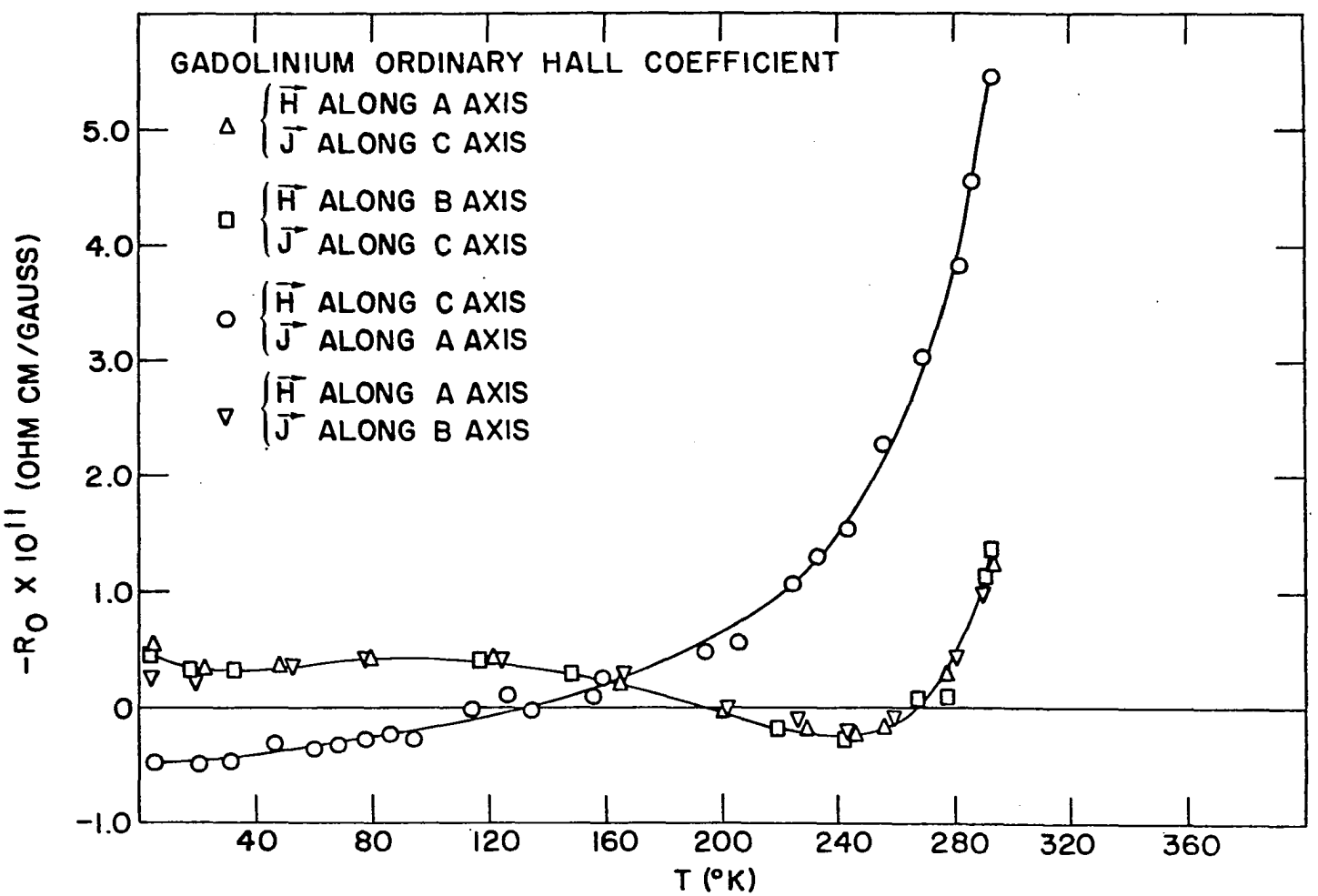

Figure 9. The ordinary Hall coefficient of gadolinium

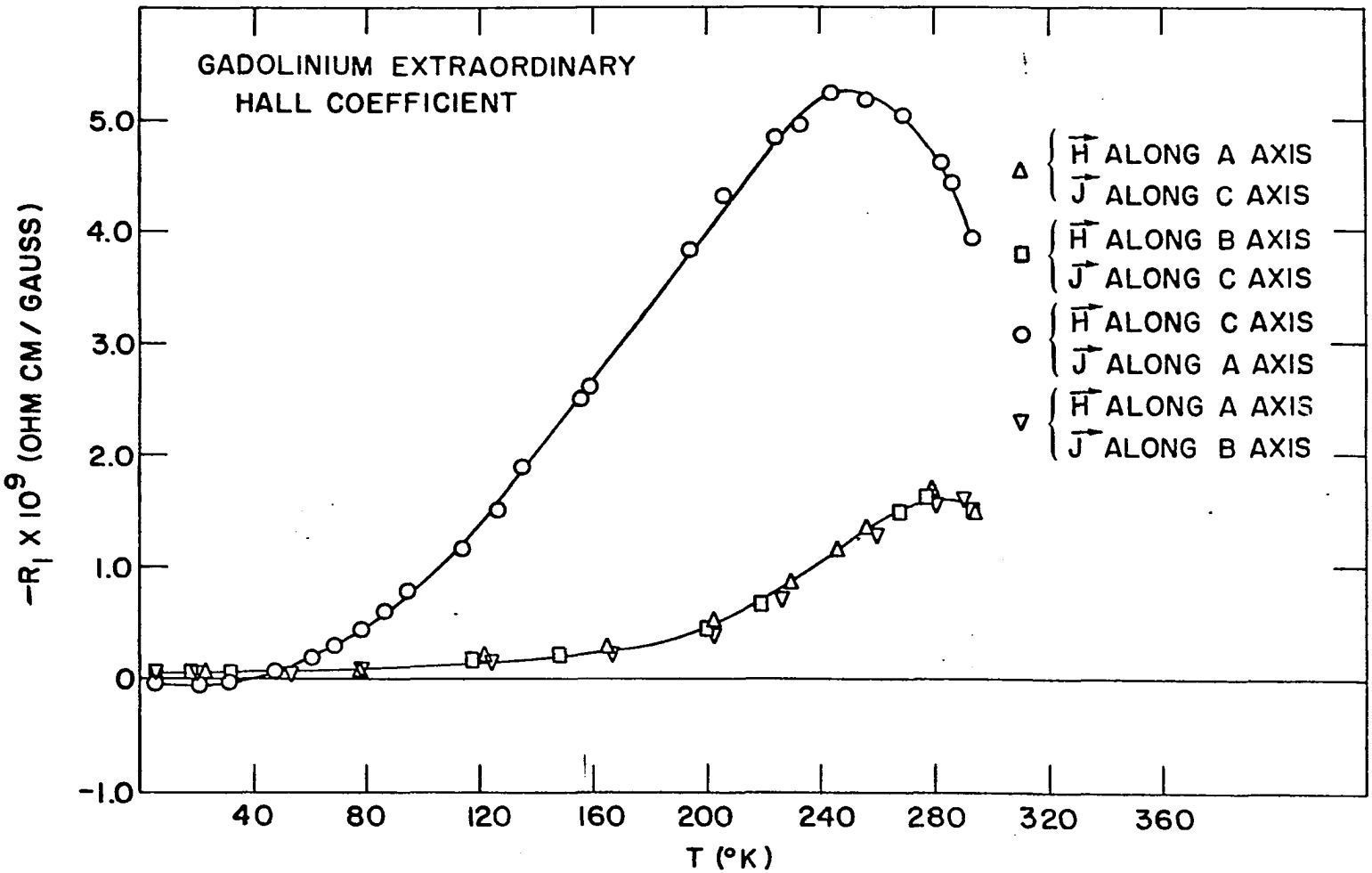

Figure 10. The extraordinary Hall coefficient of gadolinium

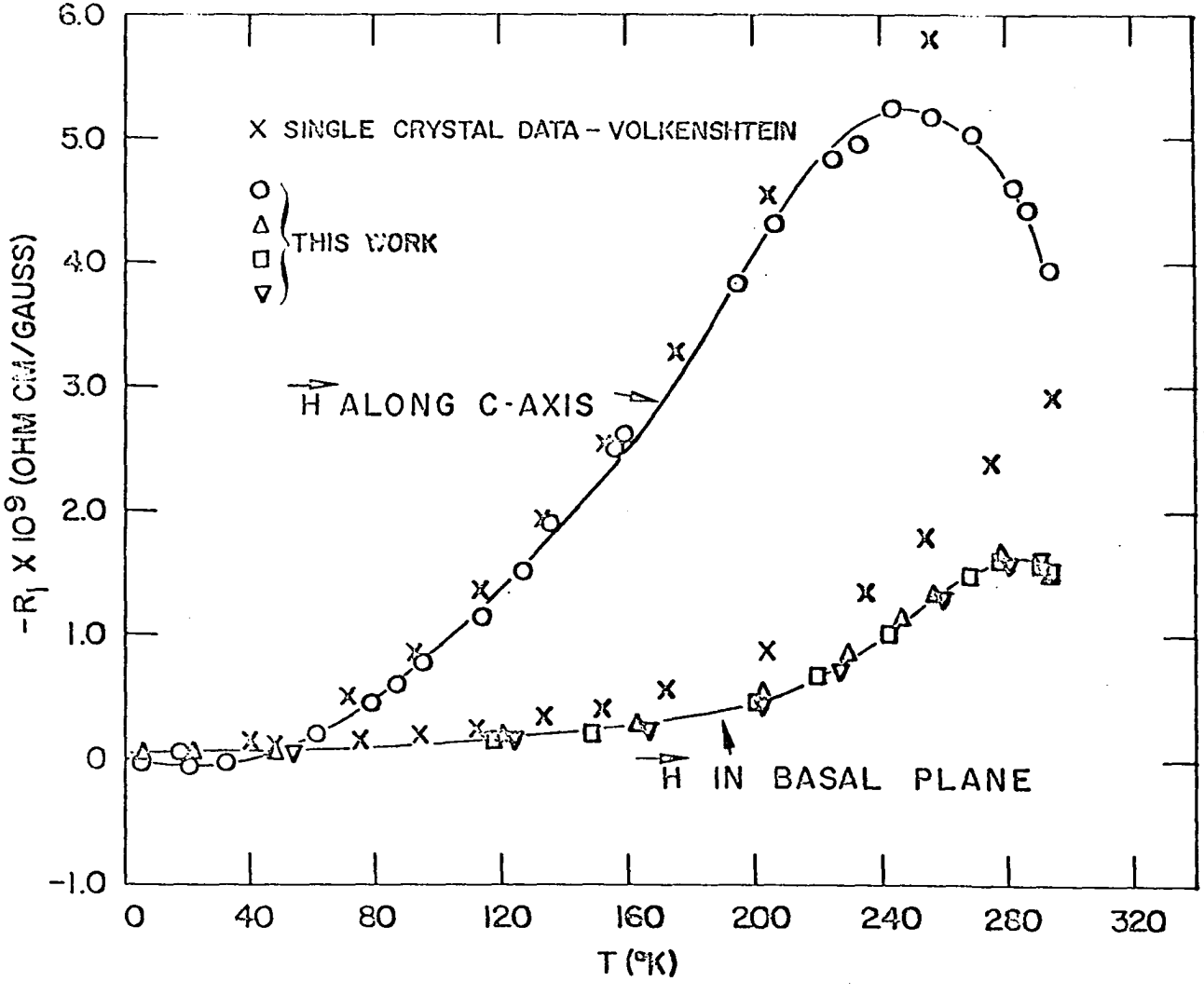

Figure 11. Comparison of the single crystal data of Volkenshtein et al. (33) with the present investigation

B. Lutetium and Yttrium

The Hall voltage, V_H, was measured for two single crystals of lutetium and two single crystals of yttrium over the temperature range from 8° to 320°K in magnetic fields up to 7.8 kOe. The orientations of the four crystals are listed in Table 2.

Table 2. Orientations of lutetium and yttrium single crystal samples

Sample	H	J	e_H	Designation
Lu I	a-axis	b-axis	c-axis	Lu a-axis
Lu II	c-axis	b-axis	a-axis	Lu c-axis
Y I	b-axis	a-axis	c-axis	Y b-axis
Y II	c-axis	a-axis	b-axis	Y c-axis

The data were taken isothermally. These measurements differ from the measurements made on gadolinium in that the Hall voltages were so small it was not practical to measure V_H as a function of H. Both lutetium and yttrium have extremely small susceptibilities, so R_o is independent of H. R_o was determined from the value of V_H at the maximum field.

Below 8°K a spurious signal was produced in the a.c. Hall effect apparatus so it was not possible to make measurements below this temperature. The explanation of this spurious signal is still a mystery, both to the author and to L. Muhlestein, who constructed the apparatus. Above 8°K the apparatus worked properly and reproduced known results for copper and silver (18). Above 320°K the adhesive used to fasten down the wires in the sample holder became soft and permitted the wires to vibrate. This introduced a spurious signal, so measurements were restricted to the range 8° to

320°K.

Figure 12 shows a plot of R_o versus T for the yttrium crystals. The interesting thing about these curves is the large anisotropy between the c-axis and basal plane, and the strong temperature dependence.

Figure 13 shows a plot of R_o versus T for the lutetium crystals. Again there is a large anisotropy and even more temperature dependence than for the yttrium crystals. Even more striking is the fact that R_o is positive for the basal plane sample. The c-axis curve for lutetium is qualitatively similar to that of yttrium.

Measurements were made on only one basal plane sample for yttrium and one for lutetium because both of these metals have hexagonal close-packed crystal structure and according to the phenomenological theory, there should be no basal plane anisotropy. This prediction was verified experimentally for gadolinium so it was not deemed necessary to measure the Hall effect in both a and b-axis samples, since they would give equivalent results.

It was not possible to measure the sign of R_o with the a.c. apparatus, so the sign of the effect was checked with the d.c. equipment. R_o was negative for both of the yttrium crystals and the c-axis lutetium crystal, but was positive for the lutetium basal plane sample.

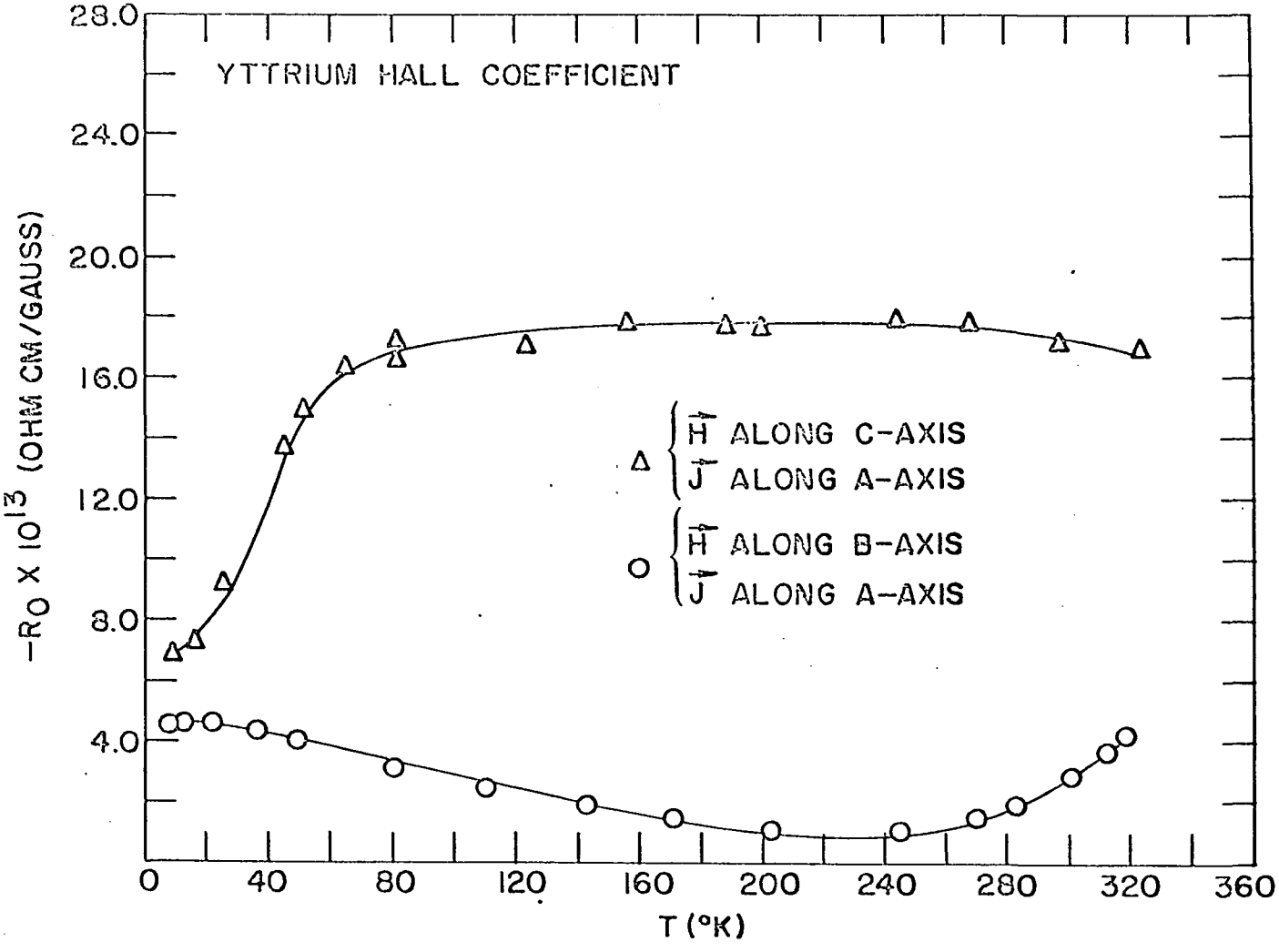

Figure 12. R_o versus T for yttrium b and c-axis crystals

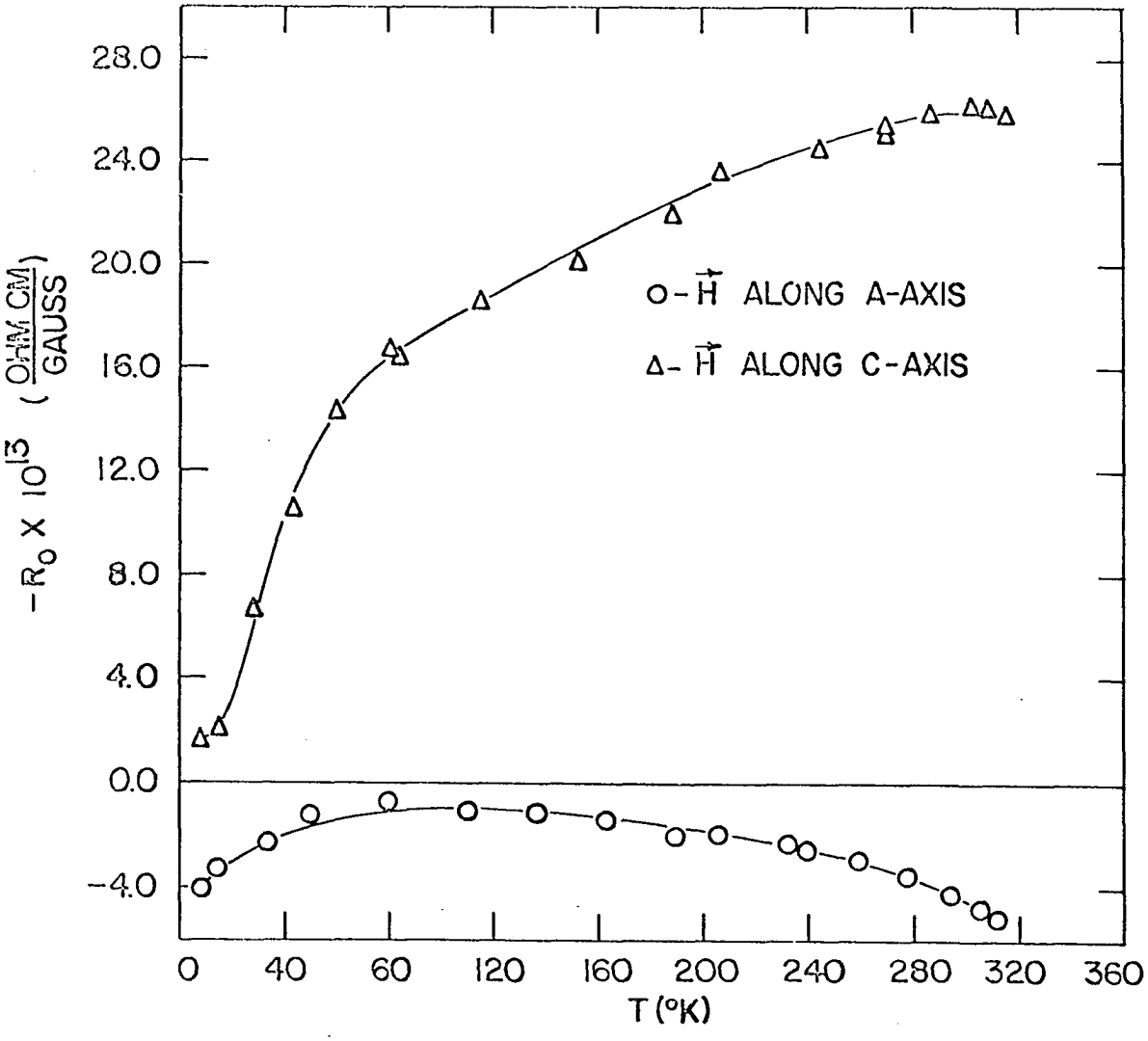

Figure 13. R_o versus T for lutetium a and c-axis crystals

V. DISCUSSION

A. Lutetium and Yttrium

The Hall effect in lutetium and yttrium will be discussed first, since these results will have a bearing on the discussion of the Hall effect in gadolinium. The features of the Hall effect in lutetium and yttrium that require discussion are the large anisotropy, the strong temperature dependence and the positive R_o observed in the lutetium basal plane sample.

The anisotropy of the Hall effect in lutetium and yttrium is almost certainly due to the extremely anisotropic Fermi surfaces of these metals. Figure 14 shows a model of the Fermi surface of gadolinium as calculated by Freeman et al. (4). Calculations by Loucks (15) and Keeton and Loucks (11) show that the Fermi surfaces of lutetium and yttrium are very similar to the Fermi surface of gadolinium in the paramagnetic state. The Fermi surface of gadolinium is thus a good approximation to the Fermi surfaces of lutetium and yttrium.

One can see from Figure 14 that the electron and hole orbits with the magnetic field applied along the c-axis will be very much different from the orbits with the field applied in the basal plane. With such different orbits for the different field directions, it is not surprising that a large anisotropy in the Hall effect is observed.

The temperature dependence of the Hall effect in lutetium and yttrium can be qualitatively understood in terms of a two-band free-electron model. The reason that a free-electron model gives qualitative results when the Fermi surface is so obviously non-spherical is that the temperature

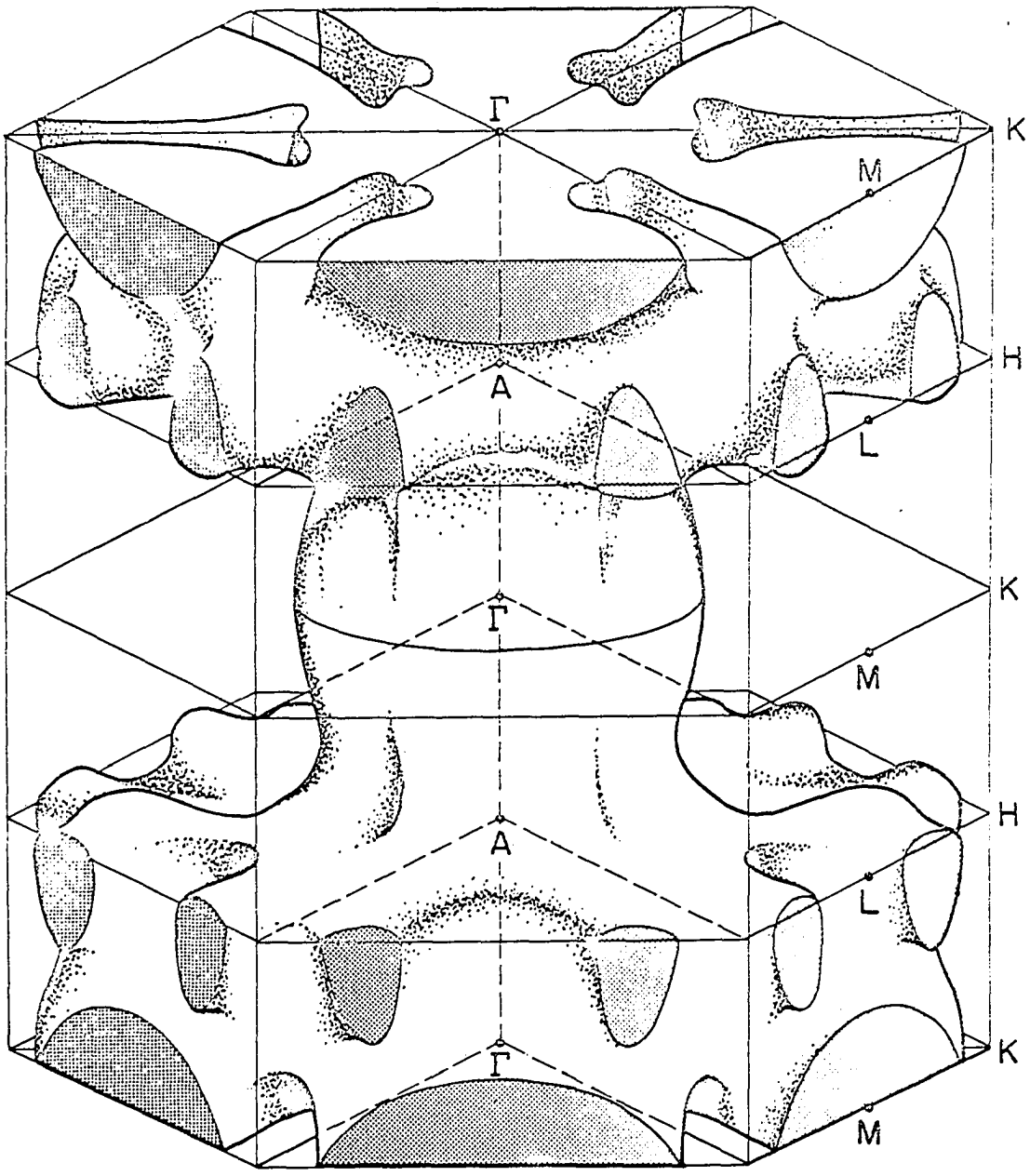

Figure 14. The complete Fermi surface for holes in gadolinium metal in the double zone representation as calculated by Freeman et al. (4)

dependence does not arise from the Fermi surface geometry. The mechanism for the temperature dependence seems to be the transition from impurity scattering at low temperatures to phonon scattering at higher temperatures. Equation 2.12 states that the Hall coefficient for a metal having two spherical Fermi surfaces, one containing n_+ holes, the other containing n_- electrons per unit volume, may be written

$$R_o = (e/\sigma^2 c)(n_+\mu_+^2 - n_-\mu_-^2) \tag{5.1}$$

where μ_+ is the hole conductivity mobility and μ_- is the electron conductivity mobility. It is reasonable to assume that the electron and hole mobilities will have different temperature dependence. We write this as

$$\mu_+ = (a + bT)^{-1} \tag{5.2}$$

$$\mu_- = (c + dT)^{-1} \quad . \tag{5.3}$$

If we substitute 5.2 and 5.3 into Equation 5.1 and assume we have a compensated metal, i.e., $n_- = n_+ = n$, we obtain

$$\text{nec } R_o = \frac{(c^2 - a^2) + 2(cd - ab)T + (d^2 - b^2)\,T^2}{(c^2 + a^2) + 2(cd + ab)T + (d^2 + b^2)\,T^2} \quad . \tag{5.4}$$

The temperature dependence of this expression is determined by the values of the coefficients a,b,c and d. One may choose initially the ratio d/b. One may then determine the ratio c/a by the relation

$$\frac{R_o(T = 0^oK)}{R_o(T = 300\ K)} = \frac{(c^2 - a^2)(d^2 + b^2)}{(c^2 + a^2)(d^2 - b^2)} \quad . \tag{5.5}$$

$R_o(T = 0)/R_o(T = 300^o)$ may be determined from the experimental data. One

may determine the ratio a/b by writing the total conductivity in terms of the electron and hole mobilities and calculating the resistivity ratio, $\rho_{4.2°K}/\rho_{300°K}$, which has been determined experimentally for each sample. Figure 15 shows the results of some calculations using Equation 5.4 and values a,b,c and d estimated as described above.

It would be pointless to try to fit these curves to the experimental data since the actual Fermi surfaces of the rare earth metals are so far from spherical, but this argument does demonstrate in a qualitative manner, a possible mechanism for the temperature dependence of R_o in yttrium and lutetium.

The difference in sign of R_o between the c-axis and a-axis lutetium samples is an interesting result. Scovil (26) reports a similar result for single crystals of titanium, where R_o is positive with the field applied along the c-axis and negative with the field applied in the basal plane. This sign change of R_o must be due to the Fermi surface geometry. One might wonder why this sign change is not also observed in yttrium, but the difference between the Hall effects in these two metals is not as drastic as one might think. From Equation 5.1 we see that for a compensated metal the sign of R_o is determined by the relative magnitudes of the electron and hole mobilities. For both lutetium and yttrium R_o is nearly zero with the field applied in the basal plane, so the electron and hole mobilities in this direction must be nearly equal. The Fermi surfaces of lutetium and yttrium are quite similar, but they are not identical so a relatively small difference in Fermi surface geometry might change the mobilities sufficiently to change the sign of R_o.

Figures 16 and 17 show R_o for polycrystalline lutetium and yttrium,

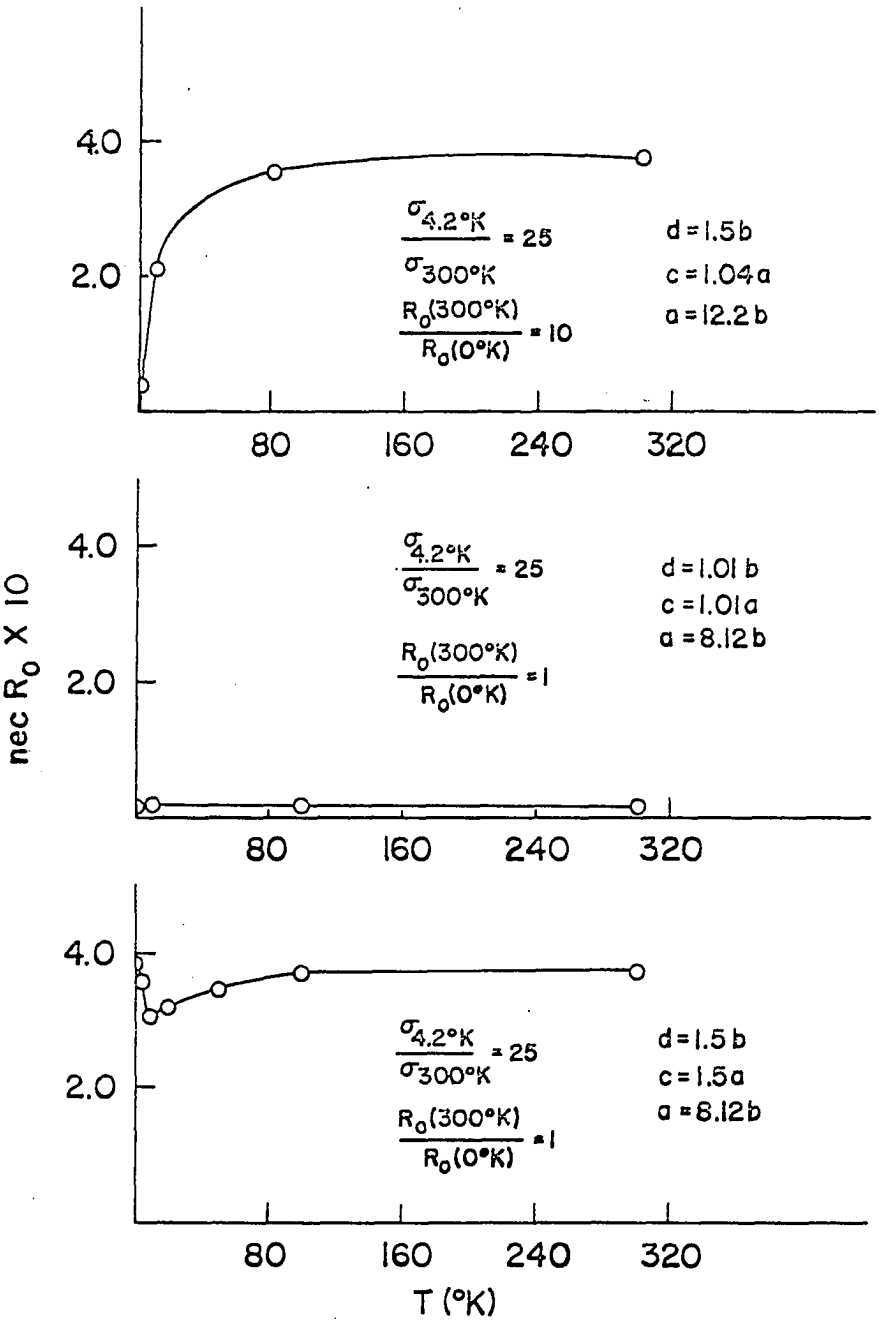

Figure 15. $necR_o$ calculated from Equation 5.4 for various values of the parameters a,b,c and d

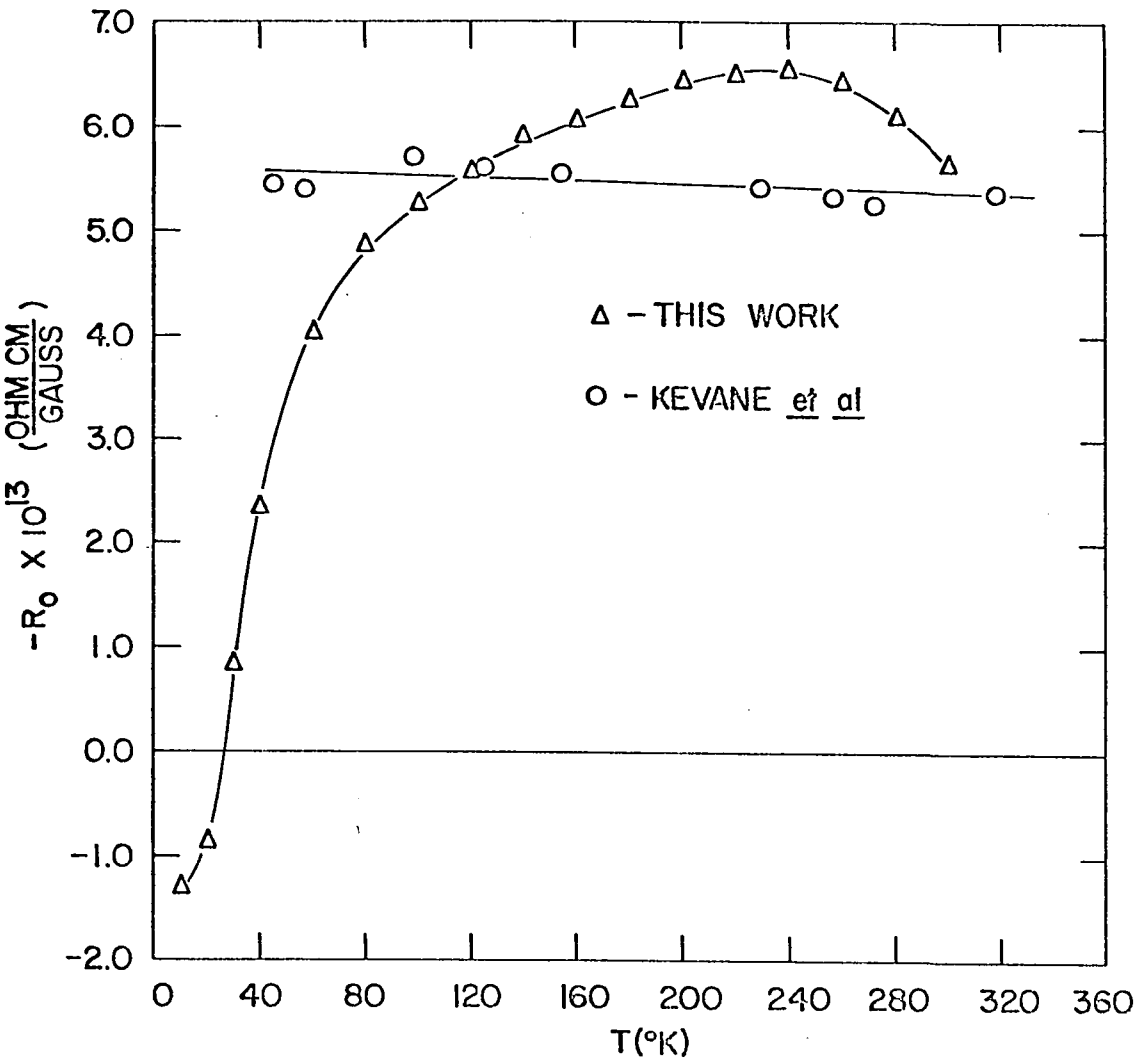

Figure 16. Comparison of R_o for lutetium, calculated from single crystal data, with the polycrystalline data of Kevane et al. (13)

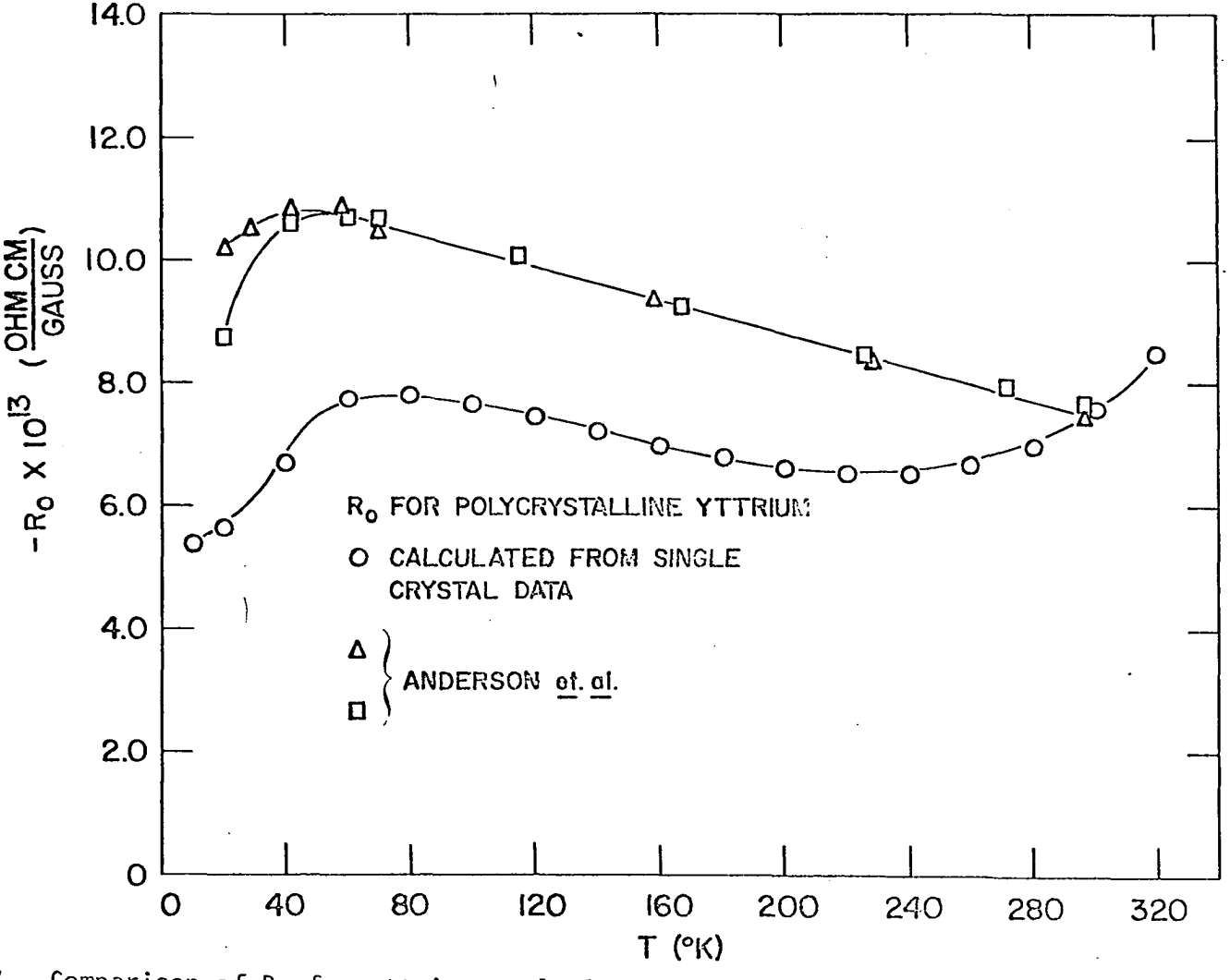

Figure 17. Comparison of R_o for yttrium, calculated from single crystal data, with the polycrystalline data of Anderson et al. (1)

calculated from the single crystal data, compared with the polycrystalline data of Kevane et al. (13) and Anderson et al. (1). The agreement is reasonably good considering the extremely small voltages being measured and the difficulty of making a polycrystalline sample with truly random orientation. Because of the large anisotropy of the Hall effect in these metals, preferred orientation in the polycrystalline specimens can change the results considerably.

B. Gadolinium

The ordinary Hall coefficient, R_0, of gadolinium also exhibits a large anisotropy and temperature dependence. In addition, R_o for gadolinium is one to two orders of magnitude larger than R_o for yttrium and lutetium over the temperature range 4.2^oK to 300^oK.

The anisotropy of the Hall effect observed in gadolinium is probably due to the anisotropic Fermi surface as was the case for yttrium and lutetium.

A two band model is not adequate to explain either the large values of R_o or the changes in sign of R_o observed in gadolinium. Kevane et al. (13) were able to interpret their polycrystalline Hall effect data above 100^oC by assuming a constant value of R_1, taking $R_o = -0.4 \times 10^{-12}$, and using the values of magnetic susceptibility of Trombe (31). These results indicate that at temperatures sufficiently high above the Curie temperature, the Hall coefficient of gadolinium is of the same order of magnitude as the Hall coefficients of yttrium and lutetium. This is what one would expect, since the electronic structures of these metals are so similar in the absence of magnetic ordering. One must conclude that the anomalously

large values of the Hall coefficient observed in gadolinium below the Curie temperature are the result of magnetic ordering.

The resistivity measurements of Nigh et al. (21) and the Seebeck effect measurements of Sill and Legvold (27) indicate that the scattering varies rather smoothly through the Curie temperature. Since the resistivity and Seebeck effect are much more sensitive to scattering than the Hall effect, one must look elsewhere to account for the behavior of R_o.

A mechanism which might provide an explanation for the anomalous behavior of R_o near and below the Curie temperature is the splitting of the conduction band of gadolinium at low temperatures through an exhange interaction with the 4f electrons. Freeman et al. (4) estimate the exchange splitting for gadolinium from their calculated density of states at the Fermi surface and the observed saturation magnetization of $7.55M_B$/atom. Their estimate is 0.61 ev. One would expect this exchange splitting to have the same temperature variation as the spontaneous magnetization. Pugh (24) proposed a similar explanation for the Hall effect in the ferromagnetic 3d transition metals.

Figure 18 shows E(k) curves for the conduction bands of gadolinium metal along the symmetry directions Γ-K-H-A. Consider the effect of the exchange splitting on the Fermi surfaces for spin-up and spin-down electrons. The dashed lines in Figure 18 are the Fermi energies for spin-up and spin-down electrons at $T = 0^oK$. Inspection of the E(k) curves in Figure 18 shows that the Fermi surface undergoes considerable distortion as the temperature is lowered, if one assumes that the E(k) curves are not themselves altered by the exchange interaction.

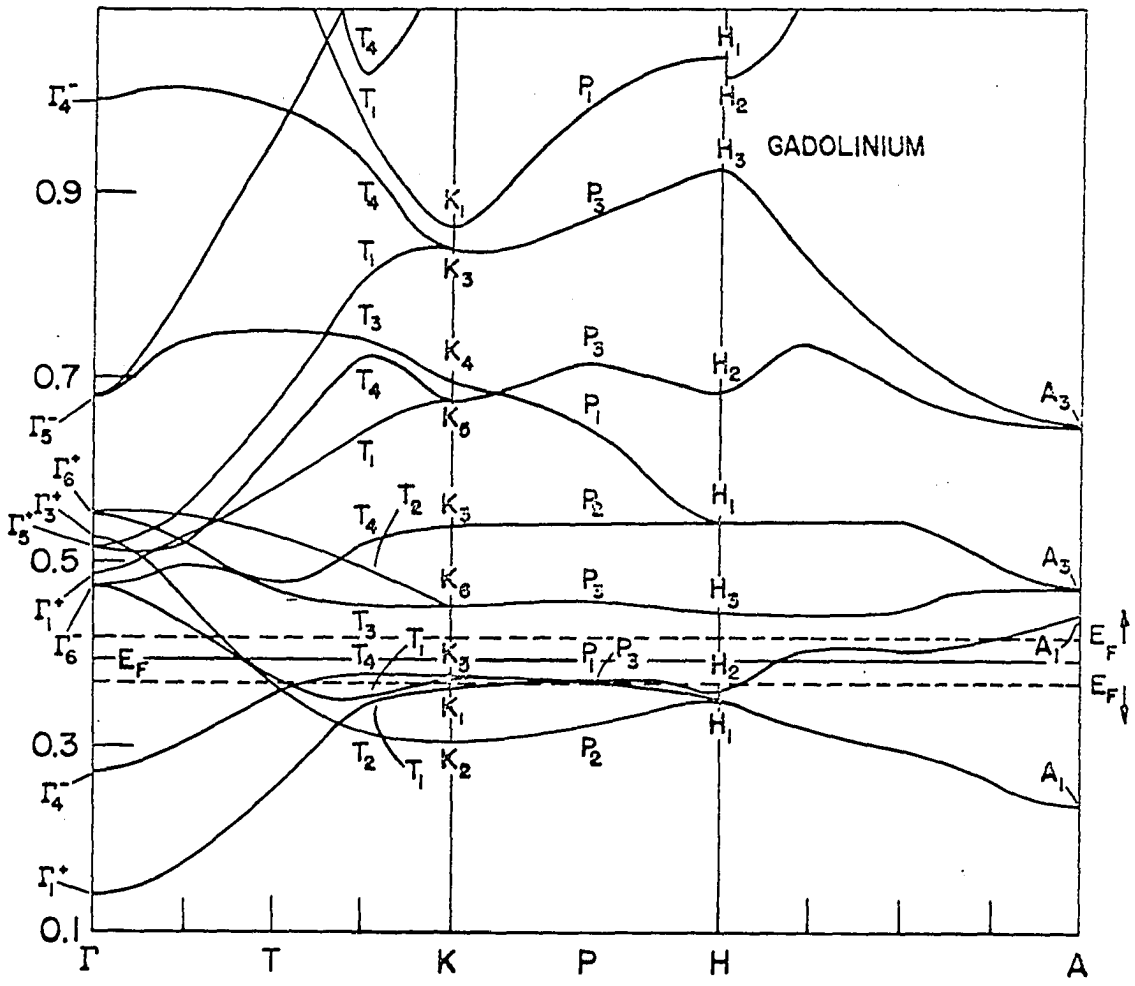

Figure 18. E(k) curves for the conduction bands of gadolinium metal along the symmetry directions Γ-K-H-A as calculated by Freeman et al. (4)

For example, the spin-up 3rd and 4th zone hole surfaces along H-A will move rapidly toward A as the temperature is lowered. Similarly, the spin-down surface will suffer considerable distortion in the region Γ-K-H.

The observed saturation magnetization of 7.55 μ_B/atom also indicates that the occupation of the spin-up and spin-down Fermi surfaces changes as the temperature is lowered.

A model based on a Fermi surface of at least four sheets would be required to account for the Hall effect in gadolinium. Even with such a model it is not feasible to calculate the temperature dependence of R_o as was done with the two band model for lutetium and yttrium. The rapidly changing Fermi surface makes it impossible to predict a reasonable temperature dependence for the mobilities of the various sheets of the Fermi surface. The picture is further complicated by the changing occupations of the spin-up and spin-down bands.

It does appear, however, that the changes in the Fermi surface caused by the exchange splitting of the conduction bands provide a possible explanation for the large magnitude and changes in sign of R_o observed in gadolinium below the Curie temperature. Relativistic calculations of the Fermi surface of gadolinium have been made recently by Keeton and Loucks (11). Their results do not differ appreciably from those of Freeman et al. (4) except that the degeneracy in the plane A-L-H is removed.

The sharp rise in R_o near the Curie temperature is somewhat peculiar, since all the other transport properties vary smoothly through the transition. The method of determining R_o and R_1 seems to still be valid near the Curie temperature, since the high-field portions of the e_H versus H

curves are still linear and a correction for the high field susceptibility has been made. It may be that R_o peaks smoothly at some temperature above the Curie temperature. Distortion of the Fermi surface from exchange splitting may still persist above the Curie temperature due to short-range ordering effects.

Figure 19 shows R_1 for the basal plane and c-axis samples plotted as a function of ρ(basal plane)$\cdot$ ρ(c-axis) and ρ^2(basal plane) respectively, where ρ is the zero field resistivity as reported by Nigh et al. (21). R_1(poly.) as calculated from the single crystal data is plotted as a function of ρ^2(poly.) in the same figure.

According to Equation 2.15, $R_1 \propto \sigma_{yx}/\sigma_{xx}\sigma_{yy} = \sigma_{yx}\rho_{xx}\rho_{yy}$. This relation is obeyed below 160°K for the c-axis sample and below 180°K for the basal plane samples. An analysis of the ρ^2 dependence of R_1 below 50°K has not been made because impurity scattering becomes important at these temperatures and resistivity measurements were not made on the same samples used for the Hall effect measurements.

R_1(poly.) versus ρ^2(poly.) shows a linear relationship from 250° to 50°K. The fact that R_1(poly.) shows a ρ^2 dependence over a much wider temperature range is probably due to an averaging of the Fermi surface effects in the polycrystalline material. Conversely, the deviation from ρ^2 dependence in the single crystal samples is probably the result of the Fermi surface changing with temperature.

The decrease in magnitude of R_1 near the Curie temperature may be due to the rapid decrease of the spontaneous magnetization in this temperature range.

Some comments regarding the single crystal data of Volkenshtein et al.

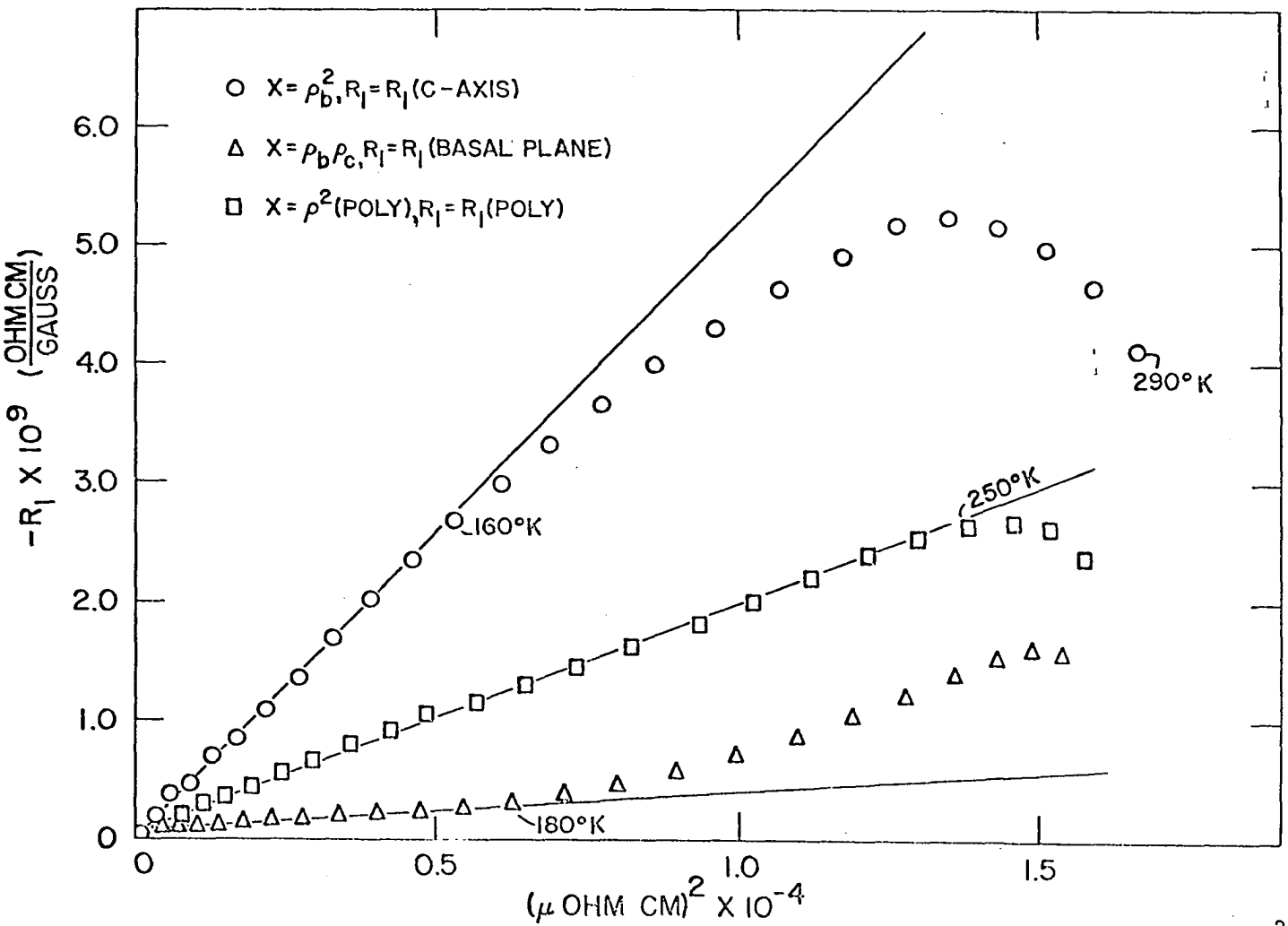

Figure 19. R_1 for the basal plane and c-axis samples versus ρ(basal plane)· ρ(c-axis) and ρ^2(basal plane) respectively; R_1(poly.) versus ρ^2(poly.)

(33) are in order, since the agreement with their results is not as good as one might hope. Their values for R_1 increase sharply near the Curie temperature instead of dropping. This seems to be the result of an erroneous equation used to calculate R_1. In an earlier paper Volkenshtein and Federov (32) calculated R_1 from the equation

$$R_1 = e_H(0) \; / \; [4\pi M_s \; (0,T)] \tag{5.6}$$

where $M_s(0,T)$ is the spontaneous magnetization. The argument used to obtain this expression is incorrect. The correct result is equation 3.10 where the quantity in the denominator is $M(\infty,T)$, the saturation magnetization. If one uses the spontaneous magnetization, as they did, R_1 will diverge at θ_c because $M_s(0,\theta_c) = 0$. Figure 20 shows a plot of $\sigma_{o,T}$ versus T and $\sigma_{\infty,T}$ versus T. $\sigma_{o,T}$ and $\sigma_{\infty,T}$ are the spontaneous magnetization per gram and the saturation magnetization per gram calculated from the data of Nigh (20). This graph illustrates the difference between using the spontaneous magnetization and using the saturation magnetization in the denominator of Equation 3.10. At lower temperatures the difference becomes less serious.

Volkenshtein et al. (33) made no correction for demagnetizing fields. This is not a large correction as regards the calculation of R_1, however their plots of e_H versus B are misleading since demagnetizing fields are very large for samples of the shape used for Hall effect measurements.

Figure 11 shows that the c-axis data of Volkenshtein et al. and the present investigation agree reasonably well except near the Curie temperature. The basal plane samples do not agree so well. It is not likely

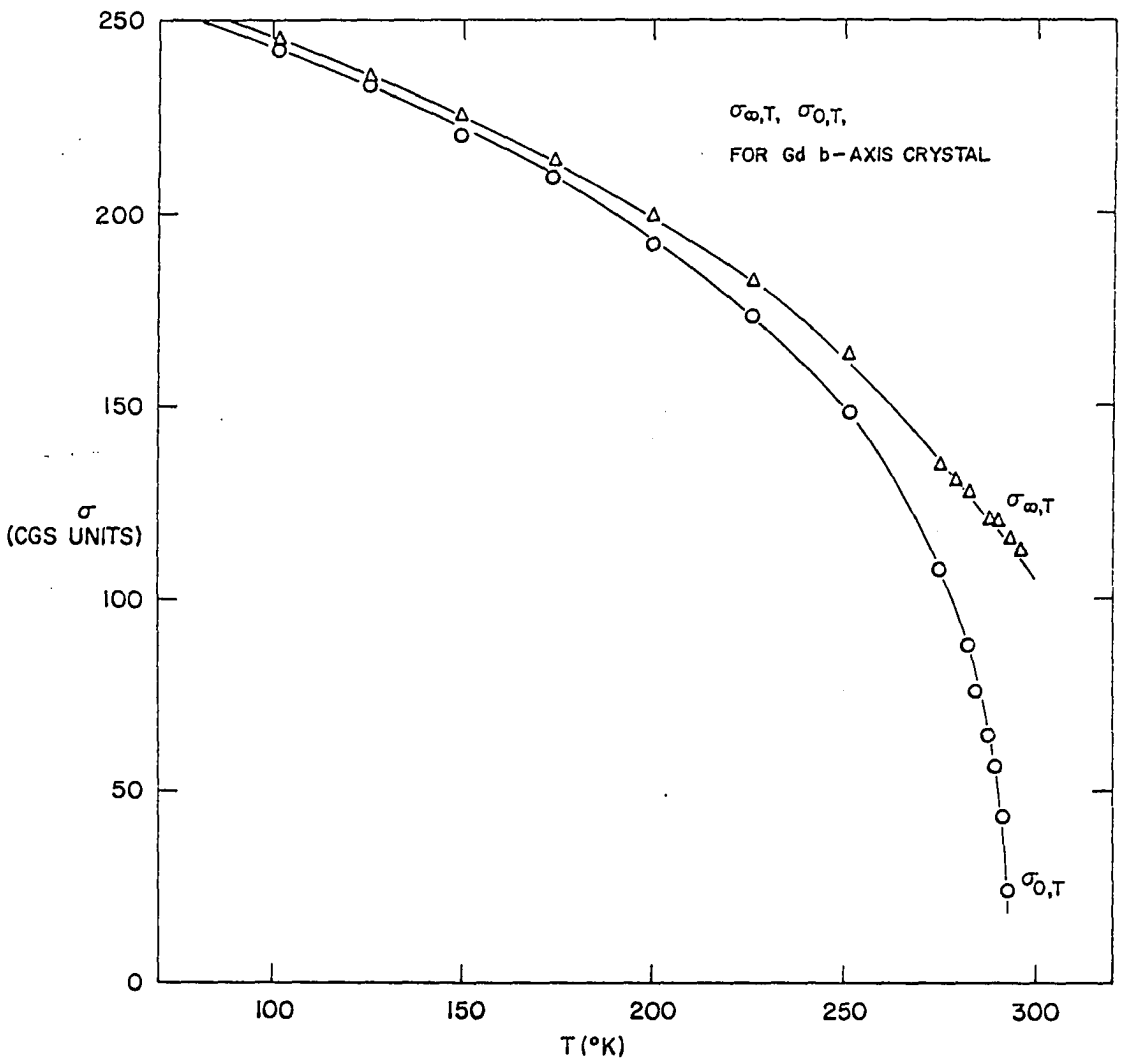

Figure 20. $\sigma_{o,T}$ versus T and $\sigma_{\infty,T}$ versus T for gadolinium single crystals

that this is due to a systematic error, since the c-axis samples agree. The results of the present investigation seem more trustworthy, however, since they were obtained from measurements on three different crystals which all yielded the same results.

It does not seem likely that magnetic anisotropy plays a large role in the anisotropy and temperature dependence of R_1. All of the information about R_1 is obtained from the e_H versus H curves for values of H above magnetic saturation. In this region there is not much anisotropy in the magnetization.

VI. BIBLIOGRAPHY

1. Anderson, G. S., S. Legvold and F. H. Spedding, Phys. Rev., 111, 1257 (1958).

2. Babushkina, N. A., Soviet Phys. - Solid State, 7, 2450 (1966).

3. Finnemore, D. K., J. E. Ostenson and T. F. Stromberg. U.S. Atomic Energy Commission Report IS-1046 [Iowa State University of Science and Technology, Ames, Iowa. Inst. for Atomic Research] (1964).

4. Freeman, A. J., J. O. Dimmock and R. E. Watson. [The augmented plane wave method and the electronic properties of rare earth metals. To be published in Löwdin, P. O., ed. ca. 1967].

5. Gurevich, L. E. and I. N. Yassievich, Soviet Phys. - Solid State, 4, 2091 (1963).

6. Jan, J. P., Solid State Physics 5, 1 (1957).

7. Jones, H. and C. Zener, Proc. Roy. Soc. (London), A145, 269 (1934).

8. Joseph, R. I. and E. Schlömann, J. Appl. Phys., 36, 1579 (1965).

9. Kagan, Yu. and L. A. Maksimov, Soviet Phys. - Solid State, 7, 422 (1965).

10. Karplus, R. and J. M. Luttinger, Phys. Rev., 95, 1154 (1954).

11. Keeton, S. and T. L. Loucks, [The relation between antiferromagnetism and the Fermi surface in some heavy rare earths.] Phys. Rev. [To be published ca. 1967].

12. Kevane, C. J., Hall effect at low temperatures for rare earth metals, unpublished Ph.D. thesis, Ames, Iowa, Library, Iowa State University of Science and Technology, 1953.

13. Kevane, C. J., S. Legvold and F. H. Spedding, Phys. Rev., 91, 1372 (1953).

14. Leribaux, H., Phys. Rev., 150, 384 (1966).

15. Loucks, T. L., Phys. Rev., 144, 504 (1966).

16. Luttinger, J. M., Phys. Rev., 112, 739 (1958).

17. Marotta, A. S. and K. J. Tauer, J. Phys. Soc. Japan, 18, 310 (1963).

18. Muhlestein, L. D., Electrical properties of metallic sodium tungsten bronze, unpublished Ph.D. thesis, Ames, Iowa, Library, Iowa State University of Science and Technology, 1966.

19. Nigh, H. E., J. Appl. Phys., 34. 3323 (1963).

20. Nigh, H. E., Magnetization and electrical resistivity of gadolinium single crystals, unpublished Ph.D. thesis, Ames, Iowa, Library, Iowa State University of Science and Technology, 1963.

21. Nigh, H. E., S. Legvold and F. H. Spedding, Phys. Rev., 132, 1092 (1963).

22. Pippard, A. B., The dynamics of conduction electrons, New York, New York, Gordon and Breach, 1965.

23. Powell, R. L., M. D. Bunch and R. J. Corruccini, Cryogenics, 1, 139 (1961).

24. Pugh, E. M., Phys. Rev., 97, 647 (1955).

25. Rhyne, J. J., Magnetostriction of dysprosium, erbium, and terbium single crystals, unpublished Ph.D. thesis, Ames, Iowa, Library, Iowa State University of Science and Technology, 1965.

26. Scovil, G. W., Appl. Phys. Letters, 9, 247 (1966).

27. Sill, L. R. and S. Legvold, Phys. Rev., 137, A1139 (1965).

28. Smit, J., Physica, 21, 877 (1955).

29. Spedding, F. J. and J. E. Powell, J. Metals, 6, 1131 (1954).

30. Strachan, C. and A. M. Murray, Proc. Phys. Soc. (London), 73, 433 (1959).

31. Trombe, F., Annales Physique, 7, 383 (1937).

32. Volkenshtein, N. V. and G. V. Federov, Phys. Metals Metallog., 18, 26 (1964).

33. Volkenshtein, N. V., G. V. Grigorova and G. V. Fyodorova, Zhur. Eksp. i Teoret. Fiz., 50, 1505 (1966).

34. Ziman, J. M., Electrons and phonons, London, England, Oxford University Press, 1960.

VII. ACKNOWLEDGEMENTS

The author wishes to express his sincere thanks to Dr. Sam Legvold for suggesting this problem and for his interest and assistance throughout the course of this investigation.

Thanks are also extended to Mr. P. Palmer and Mr. B. J. Beaudry for the preparation of the rare earth metals; to the Ames Laboratory graphics department for the preparation of the figures; to Mr. W. Sylvester and Mr. R. Brown for aid in constructing experimental apparatus and to Mr. G. Erskine for aid in maintaining the equipment and processing data.

Special thanks are extended to Dr. J. Rhyne who constructed some of the equipment used for this investigation and who was of great assistance in writing the computer programs used to process the data.

The author gratefully acknowledges the assistance of Dr. L. Muhlestein who permitted the use of his a.c. Hall effect apparatus for part of the experiment.

It is a pleasure to acknowledge the help of many of the author's Ames Laboratory colleagues: Dr. L. R. Sill for growing some of the single crystals; Mr. D. Richards, Mr. L. R. Edwards, Mr. D. Boys, Mr. W. Nellis, Mr. C. M. Cornforth, Dr. S. Keeton and Dr. R. Williams for numerous helpful discussions.

Thanks also to Dr. A. V. Gold, Dr. S. Liu and Dr. R. Fivaz for many helpful discussions.

Certainly not least has been the assistance of the author's wife, Jean, for her understanding and encouragement during the course of this investigation.

VIII. APPENDIX

A. Discussion of Errors - d.c. Method

Above magnetic saturation R_o may be determined from the equation

$$R_o = \frac{e_H(H_2) - e_H(H_1)}{H_2 - H_1} \quad , \tag{7.1}$$

where H_2 and H_1 are both larger than H_s, the field required to saturate the sample. In terms of experimentally measured quantities, Equation 7.1 may be written

$$R_o = Vt/HI \quad , \tag{7.2}$$

where $V = V(H_2) - V(H_1)$ and $H = H_2 - H_1$. The error in the measurement of R_o is thus

$$\Delta R_o/R_o = \Delta V/V + \Delta t/t - \Delta H/H - \Delta I/I \quad . \tag{7.3}$$

The estimated error in the thickness, t, is about 1%. The estimated error in the measurement of the magnetic field intensity, H, is less than 1% at fields above H_s. The estimated error in I is less than 0.1%.

The estimated error in V depends on the magnitude of V. For values of V larger than 0.2 microvolts the error is less than 5% since the potentiometer will measure to 0.01 microvolt. The error is probably considerably less than 5% because each measurement of e_H represents an average over forward and reverse current and field directions. R_o was determined by drawing a straight line through 5 to 10 points on the high field portion of the e_H versus H curve, so random errors will tend to be averaged out. For values of V less than 0.02 microvolts, corresponding to R_o of 10^{-12} or less,

one has obviously reached the limits of measurement and the relative error will be quite large. Examination of the data shows that even the very small values of R_o fit fairly smoothly onto the R_o versus T curve. The scatter of the points from a smooth curve is certainly less than 10% over almost all of the temperature range and is better than this for most of the temperatures measured.

One source of error that is very difficult to estimate for a d.c. measurement is the Ettingshausen voltage. This voltage is typically very small compared to the Hall voltage in metals. Figure 21 shows a comparison of the polycrystalline data of Kevane et al. (13) with the present investigation. The agreement is quite good over the range of temperatures where comparison is possible. Since the Ettingshausen voltage does not appear in an a.c. measurement, as was made by Kevane, this indicates that the Ettingshausen voltage does not represent a serious error.

With these considerations, the error in R_o is principally due to the error in the measurement of V.

R_1 is determined from the equation

$$R_1 = \frac{\mathcal{Q} - N\rho_m\sigma_s R_o}{\rho_m\sigma_s} \quad , \tag{7.4}$$

where ρ_m is the mass density and σ_s is the saturation magnetization per gram. $\mathcal{Q}$, the intercept of the linear portion of the e_H versus H curve on the H axis, may be determined from the equation

$$\mathcal{Q} = e_H(H_m) - R_o H_m \tag{7.5}$$

where H_m is the maximum applied field. R_1 is then given by the equation

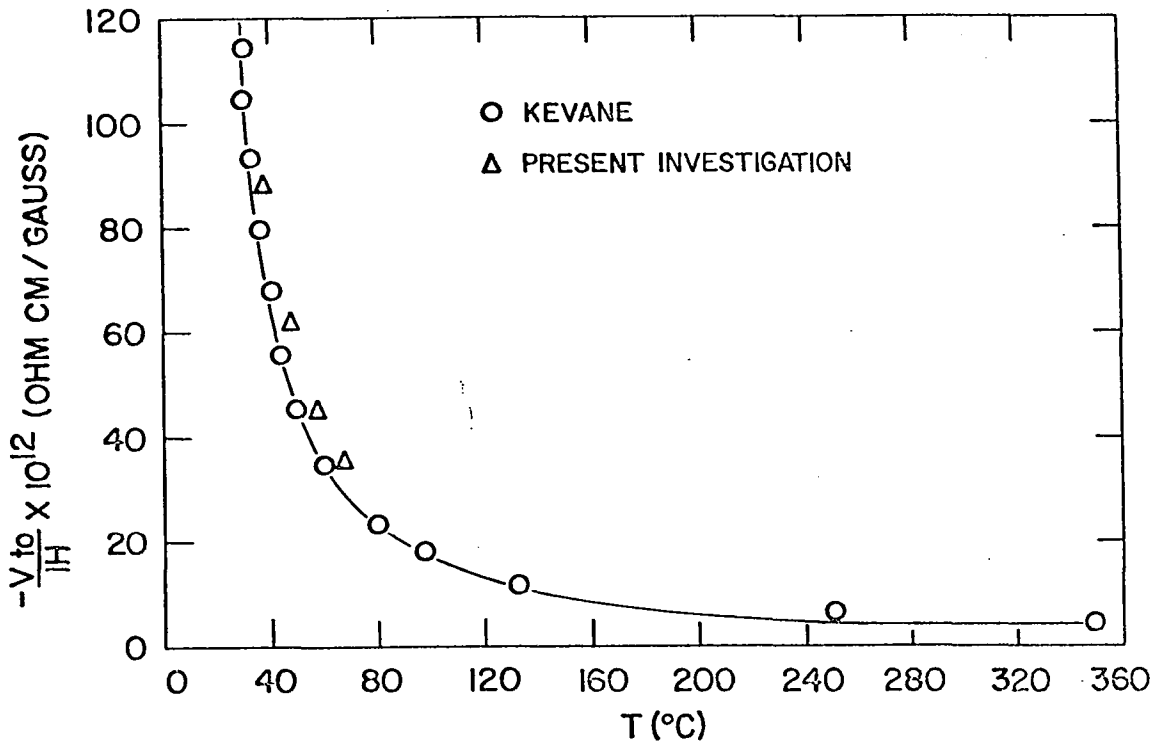

Figure 21. Comparison of the d.c. measurements on gadolinium with the a.c. measurements of Kevane et al. (13)

$$R_1 = \frac{e_H(H_m) - R_o(N\rho_m\sigma_s + H_m)}{\rho_m\sigma_s} \quad . \tag{7.6}$$

In most temperature ranges, $e_H(H_m)$ is much larger than the second term in 7.6 so the largest part of the error in R_1 will come from the measurement of e_H. Since the maximum voltage measured over almost all of the temperature range exceeded 0.5 microvolts, one can conservatively state that the error in $e_H(H_m)$ was less than 2%. In temperature ranges where the second term in 7.6 becomes comparable to e_H the error in R_1 is of the same order as the error in R_o, but this occurs only at temperatures below 100°K. The error in ρ_m is less than 0.1%. Nigh (20) estimates the error in σ_s to be less than 1%.

The temperature was controlled to within 0.1°K. Absolute accuracy of the temperature data is estimated to be $\pm$0.5°K.

B. Discussion of Errors - a.c. Method

The error in the measurement of R_o by the a.c. method is also given by Equation 7.3. The estimated error in the thickness, t, is about 1%. The estimated error in I is less than 0.1%. The estimated error in H is 1%.

The limit of resolution of the system was 10^{-9} volts and the smallest voltages measured were of the order of 10^{-8} volts, so the error in V is estimated to be less than 10% and is better than this for the c-axis lutetium and yttrium samples, where larger voltages were measured. L. Muhlestein reports (18) that his apparatus reproduced published values of R_o for copper to about 6% and reproduced published values of R_o for silver to about 7%. In both of these metals R_o is of the same order of

magnitude as for lutetium and yttrium.

C. Sample Dimensions and Demagnetizing Factors

Sample dimensions for all of the samples used in this study are listed in Table 3. Demagnetizing factors were calculated only for the gadolinium samples.

Table 3. Sample dimensions and demagnetizing factors

Sample	Length (cm)	Width (mm)	Thickness (mm)	Demag. Factor
Gd I	1.4	2.2	0.397	10.9
GD II	1.2	2.5	0.554	10.6
GD III	1.2	2.8	0.387	11.4
Gd IV	1.3	2.4	0.550	10.5
Lu I	0.77	1.6	0.634	
Lu II	0.75	1.3	0.666	
Y I	0.75	1.7	0.572	
Y II	0.75	1.8	0.504	

D. Sample Impurities

Table 4. Gadolinium impurities

Impurity	Gd I	Gd II and Gd III	Gd IV
Sm	<200	<200	<200
Y	< 20	< 20	<100
Dy	<500	<500	<500
Fe	< 30	< 30	< 30
Ni	500	500	500
Si	< 50	< 50	< 50
Ta	2000	2000	2000
Mg	< 20	< 20	< 20
Cu	< 20	< 5	< 20
W	<500	<500	<500

Table 4. (Continued)

Impurity	Gd I	Gd II and Gd III	Gd IV
Ca	< 30	< 30	< 30
Al	< 30	< 30	< 30
Cr	< 10	< 10	< 10
O_2	1611	1489	1588
H_2	1	2	3
N_2	183	181	171

Analysis was made on scraps left over after cutting out the samples. Gd II and Gd III were cut from adjacent areas of the same crystal, so analysis was made on Gd III scraps. N_2, O_2 and H_2 impurities were determined by vacuum fusion analysis. Other impurities were determined by semiquantitative spectrographic analysis and are accurate to 20%. Values quoted are in parts per million.

Table 5. Lutetium and yttrium impurities

Impurity	Lutetium	Yttrium
Er	<100	<100
Yb	< 5	<100
Tm	<100	
Sc	< 5	
Y	<300	
Tb		<200
Ho		<100
Dy		<100
Gd		<400
Sm		<200
Nd		<200
Ta	<200	<400
Mg	< 10	< 20

Table 5. (Continued)

Impurity	Lutetium	Yttrium
Fe	< 30	<100
Si	< 30	
Cu	< 10	< 70
Ni	< 10	
Al	< 30	
Ca	< 10	< 30
Cr	< 10	< 40
Ti		< 30
O_2	1024	991
N_2	45	42
H_2	46	25

Analysis was made on scraps left over after cutting out the samples. Both lutetium samples were cut from the same crystal, so only one analysis was made. This was also the case for the yttrium samples. Analysis was made by the same methods as for the gadolinium samples.

E. Tabulation of Lutetium and Yttrium Data

Table 6. Experimental data for the lutetium a-axis crystal (Lu I)

T^oK	$R_o \times 10^{13}$	T^oK	$R_o \times 10^{13}$	T^oK	$R_o \times 10^{13}$
311.4	5.11	278.6	3.68	109.9	1.06
302.4	5.06	259.0	2.90	80.8	1.00
303.3	4.82	239.5	2.52	79.8	0.70
303.6	4.97	232.3	2.28	50.0	1.21
303.6	4.74	205.4	1.94	32.8	2.32
303.6	5.00	188.8	2.02	14.4	3.32
302.9	4.72	163.2	1.63	8.8	4.04
293.6	4.28	136.0	1.14		

Table 7. Experimental data for the lutetium c-axis crystal (Lu II)

T^oK	$R_o \times 10^{13}$	T^oK	$R_o \times 10^{13}$	T^oK	$R_o \times 10^{13}$
314.8	-25.72	244.4	-24.46	80.1	-16.64
308.1	-26.04	206.2	-23.54	59.5	-14.24
301.2	-26.09	187.7	-21.87	43.0	-10.46
286.0	-25.80	151.9	-20.37	28.3	- 6.57
269.0	-25.28	144.7	-18.46	15.6	- 1.89
268.2	-24.98	83.0	-16.27	8.4	- 1.56

Table 8. Experimental data for the yttrium b-axis crystal (Y I)

T^oK	$R_o \times 10^{13}$	T^oK	$R_o \times 10^{13}$	T^oK	$R_o \times 10^{13}$
319.0	-4.20	245.4	-1.00	36.4	-4.32
312.2	-3.66	203.4	-1.06	21.7	-4.59
301.1	-2.76	171.4	-1.44	12.5	-4.50
301.1	-2.86	142.2	-1.88	7.9	-4.49
283.2	-1.93	80.6	-3.12		
270.0	-1.46	49.5	-4.05		

Table 9. Experimental data for the yttrium c-axis crystal (Y II)

T^oK	$R_o \times 10^{13}$	T^oK	$R_o \times 10^{13}$	T^oK	$R_o \times 10^{13}$
323.6	-16.90	155.8	-17.84	51.6	-14.90
296.2	-17.08	123.0	-17.00	44.8	-13.68
268.2	-17.78	80.7	-17.29	24.9	- 9.17
244.5	-17.92	80.5	-17.12	16.0	- 7.22
200.0	-17.63	80.3	-16.54	8.2	- 6.84
188.1	-17.74	64.4	-16.14		

Resistivity ratios were as follows: Lu I, 25.7; Lu II, 22.4; Y I, 15.7; Y II, 14.4.

F. Tabulation of Experimental Data for Gadolinium

The experimental data for the gadolinium single crystals are tabulated in Figures 22 - 31. These tables were printed out by the computer, so the notation requires some explanation. The quantity, E, is what was formerly called e_H, the Hall resistivity. It was not possible to print a lower case e or a subscript with the printer for the computer.

The notation -0.4689E-08 means -0.4689×10^{-8}, etc. This is again a case of having to accept what the computer was capable of printing.

Resistivity ratios were as follows: Gd I, 46; Gd II, 42; Gd IV, 34. The resistivity ratio was not measured for Gd III.

T= 4.20EG.K	
H (KOE)	E (OHM CM.)
0.0	0.0
1.0	-0.4772E-08
2.0	-0.8748E-08
3.0	-0.1352E-07
4.0	-0.1750E-07
5.0	-0.2147E-07
6.0	-0.2465E-07
8.0	-0.3420E-07
10.0	-0.4374E-07
13.0	-0.5646E-07
16.0	-0.6760E-07
20.0	-0.8668E-07
21.0	-0.9305E-07
22.0	-0.9782E-07
23.0	-0.1034E-06
24.0	-0.1113E-06
25.0	-0.1177E-06
26.0	-0.1257E-06
27.0	-0.1304E-06
28.0	-0.1352E-06
29.0	-0.1400E-06
30.0	-0.1439E-06
30.7	-0.1463E-06

T= 17.3DEG.K	
H (KOE)	E (OHM CM.)
0.0	0.0
1.0	-0.6378E-08
2.0	-0.1036E-07
3.0	-0.1435E-07
4.0	-0.1754E-07
5.0	-0.2073E-07
6.0	-0.2631E-07
8.0	-0.3428E-07
10.0	-0.4305E-07
13.0	-0.5501E-07
16.0	-0.6856E-07
20.0	-0.8530E-07
21.0	-0.9008E-07
22.0	-0.9407E-07
23.0	-0.1012E-06
24.0	-0.1060E-06
25.0	-0.1092E-06
26.0	-0.1148E-06
27.0	-0.1204E-06
28.0	-0.1236E-06
29.0	-0.1268E-06
30.0	-0.1291E-06
30.7	-0.1323E-06

T= 78.5DEG.K	
H (KOE)	E (OHM CM.)
0.0	0.0
1.0	-0.1040E-07
2.0	-0.2239E-07
3.0	-0.3679E-07
4.0	-0.4799E-07
5.0	-0.6318E-07
6.0	-0.7438E-07
8.0	-0.1008E-06
10.0	-0.1248E-06
13.0	-0.1552E-06
16.0	-0.1799E-06
20.0	-0.2071E-06
21.0	-0.2143E-06
22.0	-0.2191E-06
23.0	-0.2247E-06
24.0	-0.2295E-06
25.0	-0.2343E-06
26.0	-0.2375E-06
27.0	-0.2415E-06
28.0	-0.2447E-06
29.0	-0.2495E-06
30.0	-0.2527E-06
30.7	-0.2551E-06

T=147.6DEG.K	
H (KOE)	E (OHM CM.)
0.0	0.0
1.0	-0.2959E-07
2.0	-0.5358E-07
3.0	-0.7679E-07
4.0	-0.1016E-06
5.0	-0.1280E-06
6.0	-0.1528E-06
8.0	-0.1983E-06
10.0	-0.2415E-06
13.0	-0.2991E-06
16.0	-0.3447E-06
20.0	-0.3767E-06
21.0	-0.3823E-06
22.0	-0.3863E-06
23.0	-0.3895E-06
24.0	-0.3935E-06
25.0	-0.3959E-06
26.0	-0.3991E-06
27.0	-0.4023E-06
28.0	-0.4047E-06
29.0	-0.4079E-06
30.0	-0.4103E-06
30.7	-0.4111E-06

T=219.0DEG.K	
H (KOE)	E (OHM CM.)
0.0	0.0
1.0	-0.8790E-07
2.0	-0.1622E-06
3.0	-0.2357E-06
4.0	-0.3093E-06
5.0	-0.3836E-06
6.0	-0.4563E-06
8.0	-0.5977E-06
10.0	-0.7240E-06
13.0	-0.8726E-06
16.0	-0.9557E-06
20.0	-0.9757E-06
21.0	-0.9765E-06
22.0	-0.9757E-06
23.0	-0.9765E-06
24.0	-0.9757E-06
25.0	-0.9741E-06
26.0	-0.9725E-06
27.0	-0.9709E-06
28.0	-0.9685E-06
29.0	-0.9669E-06
30.0	-0.9653E-06
30.7	-0.9645E-06

T= 4.2DEG.K	
H (KOE)	E (OHM CM.)
0.0	0.0
1.0	-0.5567E-08
2.0	-0.1034E-07
3.0	-0.1352E-07
4.0	-0.1670E-07
5.0	-0.2147E-07
6.0	-0.2783E-07
8.0	-0.3499E-07
10.0	-0.4374E-07
13.0	-0.5805E-07
16.0	-0.6919E-07
20.0	-0.8828E-07
21.0	-0.9146E-07
22.0	-0.9702E-07
23.0	-0.1042E-06
24.0	-0.1097E-06
25.0	-0.1169E-06
27.0	-0.1296E-06
28.0	-0.1352E-06
29.0	-0.1392E-06
30.0	-0.1424E-06
30.7	-0.1455E-06

T= 32.1DEG.K	
H (KOE)	E (OHM CM.)
0.0	0.0
1.0	-0.3989E-08
2.0	-0.7978E-08
3.0	-0.1277E-07
4.0	-0.1755E-07
5.0	-0.2234E-07
6.0	-0.2713E-07
8.0	-0.3510E-07
10.0	-0.4388E-07
13.0	-0.5585E-07
16.0	-0.7021E-07
20.0	-0.8776E-07
21.0	-0.9255E-07
22.0	-0.9734E-07
23.0	-0.1021E-06
24.0	-0.1077E-06
25.0	-0.1109E-06
26.0	-0.1141E-06
27.0	-0.1181E-06
28.0	-0.1221E-06
29.0	-0.1245E-06
30.0	-0.1277E-06
30.7	-0.1292E-06

T=116.9DEG.K	
H (KOE)	E (OHM CM.)
0.0	0.0
1.0	-0.2234E-07
2.0	-0.3909E-07
3.0	-0.5904E-07
4.0	-0.7819E-07
5.0	-0.9813E-07
6.0	-0.1181E-06
8.0	-0.1564E-06
10.0	-0.1883E-06
13.0	-0.2354E-06
16.0	-0.2721E-06
20.0	-0.3096E-06
21.0	-0.3175E-06
22.0	-0.3215E-06
23.0	-0.3263E-06
24.0	-0.3319E-06
25.0	-0.3351E-06
26.0	-0.3399E-06
27.0	-0.3431E-06
28.0	-0.3471E-06
29.0	-0.3510E-06
30.0	-0.3550E-06
30.7	-0.3574E-06

T=200.3DEG.K	
H (KOE)	E (OHM CM.)
0.0	0.0
1.0	-0.6003E-07
2.0	-0.1073E-06
3.0	-0.1577E-06
4.0	-0.2049E-06
5.0	-0.2545E-06
6.0	-0.3042E-06
8.0	-0.3986E-06
10.0	-0.4890E-06
13.0	-0.6027E-06
16.0	-0.6811E-06
20.0	-0.7076E-06
21.0	-0.7109E-06
22.0	-0.7108E-06
23.0	-0.7108E-06
24.0	-0.7108E-06
25.0	-0.7108E-06
26.0	-0.7108E-06
27.0	-0.7108E-06
28.0	-0.7108E-06
29.0	-0.7108E-06
30.0	-0.7092E-06
30.7	-0.7084E-06

T=241.8DEG.K	
H (KOE)	E (OHM CM.)
0.0	0.0
1.0	-0.1304E-06
2.0	-0.2375E-06
3.0	-0.3479E-06
4.0	-0.4559E-06
5.0	-0.5654E-06
6.0	-0.6718E-06
8.0	-0.8821E-06
10.0	-0.1068E-05
13.0	-0.1271E-05
16.0	-0.1334E-05
20.0	-0.1340E-05
21.0	-0.1340E-05
22.0	-0.1337E-05
23.0	-0.1337E-05
24.0	-0.1333E-05
25.0	-0.1330E-05
26.0	-0.1327E-05
27.0	-0.1324E-05
28.0	-0.1322E-05
29.0	-0.1320E-05
30.0	-0.1319E-05
30.7	-0.1316E-05

Figure 22. Experimental data for the gadolinium b-axis sample (Gd I)

T=267.4DEG.K

H (KOE)	E (OHM CM.)
0.0	0.0
1.0	-0.1953E-06
2.0	-0.3538E-06
3.0	-0.5115E-06
4.0	-0.6683E-06
5.0	-0.8268E-06
6.0	-0.9789E-06
8.0	-0.1269E-05
10.0	-0.1499E-05
13.0	-0.1642E-05
16.0	-0.1674E-05
20.0	-0.1697E-05
21.0	-0.1701E-05
22.0	-0.1704E-05
23.0	-0.1706E-05
24.0	-0.1707E-05
25.0	-0.1709E-05
26.0	-0.1711E-05
27.0	-0.1714E-05
28.0	-0.1714E-05
29.0	-0.1717E-05
30.0	-0.1718E-05
30.7	-0.1717E-05

T=276.7DEG.K

H (KOE)	E (OHM CM.)
0.0	0.0
1.0	-0.2207E-06
2.0	-0.3959E-06
3.0	-0.5702E-06
4.0	-0.7414E-06
5.0	-0.9133E-06
6.0	-0.1076E-05
8.0	-0.1368E-05
10.0	-0.1552E-05
13.0	-0.1634E-05
16.0	-0.1675E-05
20.0	-0.1718E-05
21.0	-0.1727E-05
22.0	-0.1734E-05
23.0	-0.1739E-05
24.0	-0.1743E-05
25.0	-0.1749E-05
26.0	-0.1751E-05
27.0	-0.1755E-05
28.0	-0.1759E-05
29.0	-0.1761E-05
30.0	-0.1761E-05
30.7	-0.1762E-05

T=290.0DEG.K

H (KOE)	E (OHM CM.)
0.0	0.0
1.0	-0.2271E-06
2.0	-0.4127E-06
3.0	-0.5926E-06
4.0	-0.7606E-06
5.0	-0.9037E-06
6.0	-0.1006E-05
8.0	-0.1151E-05
10.0	-0.1250E-05
13.0	-0.1365E-05
16.0	-0.1445E-05
20.0	-0.1533E-05
21.0	-0.1551E-05
22.0	-0.1568E-05
23.0	-0.1585E-05
24.0	-0.1600E-05
25.0	-0.1610E-05
26.0	-0.1628E-05
27.0	-0.1639E-05
28.0	-0.1649E-05
29.0	-0.1661E-05
30.0	-0.1674E-05
30.7	-0.1679E-05

T=291.5DEG.K

H (KOE)	E (OHM CM.)
0.0	0.0
1.0	-0.2265E-06
2.0	-0.4074E-06
3.0	-0.5827E-06
4.0	-0.7300E-06
5.0	-0.8492E-06
6.0	-0.9437E-06
8.0	-0.1101E-05
10.0	-0.1220E-05
13.0	-0.1349E-05
16.0	-0.1433E-05
20.0	-0.1521E-05
21.0	-0.1542E-05
22.0	-0.1560E-05
23.0	-0.1581E-05
24.0	-0.1596E-05
25.0	-0.1612E-05
26.0	-0.1632E-05
27.0	-0.1654E-05
28.0	-0.1670E-05
29.0	-0.1686E-05
30.0	-0.1702E-05
30.7	-0.1712E-05

T=292.3DEG.K

H (KOE)	E (OHM CM.)
0.0	0.0
1.0	-0.2249E-06
2.0	-0.4018E-06
3.0	-0.5627E-06
4.0	-0.7011E-06
5.0	-0.8172E-06
6.0	-0.9141E-06
8.0	-0.1069E-05
10.0	-0.1181E-05
13.0	-0.1306E-05
16.0	-0.1409E-05
20.0	-0.1524E-05
21.0	-0.1546E-05
22.0	-0.1566E-05
23.0	-0.1583E-05
24.0	-0.1598E-05
25.0	-0.1613E-05
26.0	-0.1631E-05
27.0	-0.1649E-05
28.0	-0.1665E-05
29.0	-0.1678E-05
30.0	-0.1695E-05
30.7	-0.1708E-05

T=295.6DEG.K

H (KOE)	E (OHM CM.)
0.0	0.0
1.0	-0.1785E-06
2.0	-0.3186E-06
3.0	-0.4498E-06
4.0	-0.5667E-06
5.0	-0.6739E-06
6.0	-0.7636E-06
8.0	-0.9085E-06
10.0	-0.1025E-05
13.0	-0.1176E-05
16.0	-0.1297E-05
20.0	-0.1415E-05
21.0	-0.1441E-05
22.0	-0.1464E-05
23.0	-0.1485E-05
24.0	-0.1510E-05
25.0	-0.1534E-05
26.0	-0.1554E-05
27.0	-0.1572E-05
28.0	-0.1587E-05
29.0	-0.1601E-05
30.0	-0.1614E-05
30.7	-0.1623E-05

T=300.7DEG.K

H (KOE)	E (OHM CM.)
0.0	0.0
1.0	-0.1058E-06
2.0	-0.2042E-06
3.0	-0.3010E-06
4.0	-0.3913E-06
5.0	-0.4800E-06
6.0	-0.5589E-06
8.0	-0.7070E-06
10.0	-0.8282E-06
13.0	-0.9876E-06
16.0	-0.1115E-05
20.0	-0.1253E-05
25.0	-0.1381E-05
30.7	-0.1500E-05

T=301.5DEG.K

H (KOE)	E (OHM CM.)
0.0	0.0
1.0	0.1151E-06
2.0	0.2085E-06
3.0	0.3002E-06
4.0	0.3872E-06
5.0	0.4733E-06
6.0	0.5506E-06
8.0	0.6995E-06
10.0	0.8235E-06
13.0	0.9804E-06
16.0	0.1112E-05
20.0	0.1251E-05
25.0	0.1379E-05
30.7	0.1509E-05

T=307.8DEG.K

H (KOE)	E (OHM CM.)
0.0	0.0
1.0	-0.7078E-07
2.0	-0.1407E-06
3.0	-0.1961E-06
4.0	-0.2717E-06
5.0	-0.3344E-06
6.0	-0.3946E-06
8.0	-0.5125E-06
10.0	-0.6256E-06
13.0	-0.7785E-06
16.0	-0.8989E-06
20.0	-0.1048E-05
25.0	-0.1206E-05
30.1	-0.1327E-05

T=310.3DEG.K

H (KOE)	E (OHM CM.)
0.0	0.0
1.0	-0.6878E-07
2.0	-0.1288E-06
3.0	-0.1879E-06
4.0	-0.2471E-06
5.0	-0.3039E-06
6.0	-0.3615E-06
8.0	-0.4695E-06
10.0	-0.5759E-06
13.0	-0.7142E-06
16.0	-0.8445E-06
20.0	-0.9973E-06
25.0	-0.1151E-05
30.7	-0.1309E-05

T=310.6DEG.K

H (KOE)	E (OHM CM.)
0.0	0.0
1.0	-0.6101E-07
2.0	-0.1269E-06
3.0	-0.1855E-06
4.0	-0.2424E-06
5.0	-0.3010E-06
6.0	-0.3539E-06
8.0	-0.4629E-06
10.0	-0.5573E-06
13.0	-0.7029E-06
16.0	-0.8200E-06
20.0	-0.9884E-06
25.0	-0.1128E-05
30.7	-0.1276E-05

T=320.2DEG.K

H (KOE)	E (OHM CM.)
0.0	0.0
1.0	-0.4983E-07
2.0	-0.9001E-07
3.0	-0.1302E-06
4.0	-0.1712E-06
5.0	-0.2130E-06
6.0	-0.2515E-06
8.0	-0.3335E-06
10.0	-0.4107E-06
13.0	-0.5240E-06
16.0	-0.6276E-06
20.0	-0.7611E-06
25.0	-0.9065E-06
30.7	-0.1050E-05

Figure 23. Experimental data for the gadolinium b-axis sample (Gd I)

T=329.5DEG.K

H (KOE)	E (OHM CM.)
0.0	0.0
1.0	-0.3173E-07
2.0	-0.6427E-07
3.0	-0.9681E-07
4.0	-0.1277E-06
5.0	-0.1595E-06
6.0	-0.1904E-06
8.0	-0.2530E-06
10.0	-0.3148E-06
13.0	-0.4011E-06
16.0	-0.4897E-06
20.0	-0.5996E-06
25.0	-0.7273E-06
30.7	-0.8729E-06

T=342.1DEG.K

H (KOE)	E (OHM CM.)
0.0	0.0
1.0	-0.2440E-07
2.0	-0.5126E-07
3.0	-0.7159E-07
4.0	-0.9600E-07
5.0	-0.1204E-06
6.0	-0.1440E-06
8.0	-0.1879E-06
10.0	-0.2367E-06
13.0	-0.3018E-06
16.0	-0.3750E-06
20.0	-0.4588E-06
25.0	-0.5687E-06
30.7	-0.6842E-06

T=341.5DEG.K

H (KOE)	E (OHM CM.)
0.0	0.0
1.0	-0.5047E-07
2.0	-0.8811E-07
3.0	-0.1250E-06
4.0	-0.1602E-06
5.0	-0.1987E-06
6.0	-0.2347E-06
8.0	-0.3108E-06
10.0	-0.3845E-06
13.0	-0.4942E-06
16.0	-0.6024E-06
20.0	-0.7474E-06
21.0	-0.7850E-06
22.0	-0.8203E-06
23.0	-0.8539E-06
24.0	-0.8892E-06
25.0	-0.9244E-06
26.0	-0.9589E-06
27.0	-0.9941E-06
28.0	-0.1029E-05
29.0	-0.1063E-05
30.0	-0.1097E-05
30.7	-0.1122E-05

Figure 24. Experimental data for the gadolinium b-axis sample (Gd I)

T= 4.7DEG.K	
H (KOE)	E (OHM CM.)
0.0	0.0
1.0	-0.1203E-07
2.0	-0.1094E-07
3.0	-0.1869E-07
4.0	-0.2407E-07
5.0	-0.2844E-07
6.0	-0.3282E-07
8.0	-0.4157E-07
10.0	-0.4923E-07
13.0	-0.6345E-07
16.0	-0.7877E-07
20.0	-0.1017E-06
21.0	-0.1083E-06
22.0	-0.1160E-06
23.0	-0.1203E-06
24.0	-0.1247E-06
25.0	-0.1291E-06
26.0	-0.1346E-06
27.0	-0.1378E-06
28.0	-0.1422E-06
29.0	-0.1466E-06
30.0	-0.1488E-06
30.7	-0.1521E-06

T= 53.4DEG.K	
H (KOE)	E (OHM CM.)
0.0	0.0
1.0	-0.1203E-07
2.0	-0.1641E-07
3.0	-0.2516E-07
4.0	-0.3173E-07
5.0	-0.3829E-07
6.0	-0.4485E-07
8.0	-0.5689E-07
10.0	-0.6892E-07
13.0	-0.8861E-07
16.0	-0.9955E-07
20.0	-0.1247E-06
21.0	-0.1302E-06
22.0	-0.1357E-06
23.0	-0.1389E-06
24.0	-0.1455E-06
25.0	-0.1477E-06
26.0	-0.1521E-06
27.0	-0.1553E-06
28.0	-0.1597E-06
29.0	-0.1630E-06
30.0	-0.1663E-06
30.7	-0.1696E-06

T=122.7DEG.K	
H (KOE)	E (OHM CM.)
0.0	0.0
1.0	-0.2188E-07
2.0	-0.4704E-07
3.0	-0.6673E-07
4.0	-0.7877E-07
5.0	-0.9189E-07
6.0	-0.1050E-06
8.0	-0.1346E-06
10.0	-0.1707E-06
13.0	-0.2243E-06
16.0	-0.2680E-06
20.0	-0.3085E-06
21.0	-0.3162E-06
22.0	-0.3249E-06
23.0	-0.3304E-06
24.0	-0.3369E-06
25.0	-0.3402E-06
26.0	-0.3446E-06
27.0	-0.3512E-06
28.0	-0.3555E-06
29.0	-0.3599E-06
30.0	-0.3643E-06
30.7	-0.3676E-06

T=166.3DEG.K	
H (KOE)	E (OHM CM.)
0.0	0.0
1.0	-0.4048E-07
2.0	-0.6673E-07
3.0	-0.9955E-07
4.0	-0.1160E-06
5.0	-0.1324E-06
6.0	-0.1543E-06
8.0	-0.2046E-06
10.0	-0.2505E-06
13.0	-0.3118E-06
16.0	-0.3687E-06
20.0	-0.4157E-06
21.0	-0.4245E-06
22.0	-0.4288E-06
23.0	-0.4332E-06
24.0	-0.4387E-06
25.0	-0.4431E-06
26.0	-0.4474E-06
27.0	-0.4496E-06
28.0	-0.4529E-06
29.0	-0.4573E-06
30.0	-0.4595E-06
30.7	-0.4617E-06

T=202.4DEG.K	
H (KOE)	E (OHM CM.)
0.0	0.0
1.0	-0.8862E-07
2.0	-0.1389E-06
3.0	-0.1860E-06
4.0	-0.2243E-06
5.0	-0.2735E-06
6.0	-0.3205E-06
8.0	-0.4113E-06
10.0	-0.4923E-06
13.0	-0.5929E-06
16.0	-0.6575E-06
20.0	-0.7045E-06
21.0	-0.7089E-06
22.0	-0.7144E-06
23.0	-0.7177E-06
24.0	-0.7198E-06
25.0	-0.7220E-06
26.0	-0.7231E-06
27.0	-0.7242E-06
28.0	-0.7264E-06
29.0	-0.7264E-06
30.0	-0.7275E-06
30.7	-0.7275E-06

T= 19.9DEG.K	
H (KOE)	E (OHM CM.)
0.0	0.0
1.0	-0.5470E-08
2.0	-0.9846E-08
3.0	-0.1422E-07
4.0	-0.1969E-07
5.0	-0.2189E-07
6.0	-0.2735E-07
8.0	-0.3501E-07
10.0	-0.4485E-07
13.0	-0.5689E-07
16.0	-0.6783E-07
20.0	-0.8752E-07
21.0	-0.9299E-07
22.0	-0.9627E-07
23.0	-0.1006E-06
24.0	-0.1061E-06
25.0	-0.1072E-06
26.0	-0.1105E-06
27.0	-0.1149E-06
28.0	-0.1182E-06
29.0	-0.1203E-06
30.0	-0.1225E-06
30.7	-0.1247E-06

T= 78.1DEG.K	
H (KOE)	E (OHM CM.)
0.0	0.0
1.0	-0.1313E-07
2.0	-0.2516E-07
3.0	-0.3501E-07
4.0	-0.4485E-07
5.0	-0.5361E-07
6.0	-0.6345E-07
8.0	-0.8205E-07
10.0	-0.1006E-06
13.0	-0.1269E-06
16.0	-0.1521E-06
20.0	-0.1882E-06
21.0	-0.1947E-06
22.0	-0.2002E-06
23.0	-0.2068E-06
24.0	-0.2122E-06
25.0	-0.2166E-06
26.0	-0.2221E-06
27.0	-0.2265E-06
28.0	-0.2319E-06
29.0	-0.2352E-06
30.0	-0.2385E-06
30.7	-0.2429E-06

T=124.8DEG.K	
H (KOE)	E (OHM CM.)
0.0	0.0
1.0	-0.2079E-07
2.0	-0.3501E-07
3.0	-0.4485E-07
4.0	-0.5798E-07
5.0	-0.7549E-07
6.0	-0.8971E-07
8.0	-0.1225E-06
10.0	-0.1499E-06
13.0	-0.1925E-06
16.0	-0.2297E-06
20.0	-0.2724E-06
21.0	-0.2812E-06
22.0	-0.2888E-06
23.0	-0.2954E-06
24.0	-0.3019E-06
25.0	-0.3096E-06
26.0	-0.3162E-06
27.0	-0.3216E-06
28.0	-0.3271E-06
29.0	-0.3337E-06
30.0	-0.3380E-06
30.7	-0.3435E-06

T=193.2DEG.K	
H (KOE)	E (OHM CM.)
0.0	0.0
1.0	-0.5908E-07
2.0	-0.9080E-07
3.0	-0.1269E-06
4.0	-0.1597E-06
5.0	-0.1947E-06
6.0	-0.2254E-06
8.0	-0.2888E-06
10.0	-0.3435E-06
13.0	-0.4157E-06
16.0	-0.4770E-06
20.0	-0.5295E-06
21.0	-0.5393E-06
22.0	-0.5470E-06
23.0	-0.5547E-06
24.0	-0.5601E-06
25.0	-0.5656E-06
26.0	-0.5689E-06
27.0	-0.5722E-06
28.0	-0.5776E-06
29.0	-0.5798E-06
30.0	-0.5831E-06
30.7	-0.5842E-06

T=226.5DEG.K	
H (KOE)	E (OHM CM.)
0.0	0.0
1.0	-0.9627E-07
2.0	-0.1608E-06
3.0	-0.2265E-06
4.0	-0.2943E-06
5.0	-0.3720E-06
6.0	-0.4529E-06
8.0	-0.5973E-06
10.0	-0.7253E-06
13.0	-0.8796E-06
16.0	-0.9715E-06
20.0	-0.1014E-05
21.0	-0.1020E-05
22.0	-0.1022E-05
23.0	-0.1024E-05
24.0	-0.1027E-05
25.0	-0.1026E-05
26.0	-0.1027E-05
27.0	-0.1028E-05
28.0	-0.1027E-05
29.0	-0.1028E-05
30.0	-0.1027E-05
30.7	-0.1026E-05

Figure 25. Experimental data for a gadolinium a-axis sample (Gd II)

T=242.5DEG.K	
H (KOE)	E (OHM CM.)
0.0	0.0
1.0	-0.1476E-06
2.0	-0.2460E-06
3.0	-0.3432E-06
4.0	-0.4362E-06
5.0	-0.5280E-06
6.0	-0.6143E-06
8.0	-0.7739E-06
10.0	-0.9095E-06
13.0	-0.1067E-05
16.0	-0.1162E-05
20.0	-0.1223E-05
21.0	-0.1231E-05
22.0	-0.1236E-05
23.0	-0.1243E-05
24.0	-0.1246E-05
25.0	-0.1249E-05
26.0	-0.1252E-05
27.0	-0.1254E-05
28.0	-0.1256E-05
29.0	-0.1256E-05
30.0	-0.1257E-05
30.7	-0.1259E-05

T=259.9DEG.K	
H (KOE)	E (OHM CM.)
0.0	0.0
1.0	-0.1860E-06
2.0	-0.3184E-06
3.0	-0.4496E-06
4.0	-0.5820E-06
5.0	-0.7155E-06
6.0	-0.8489E-06
8.0	-0.1101E-05
10.0	-0.1293E-05
13.0	-0.1464E-05
16.0	-0.1529E-05
20.0	-0.1561E-05
21.0	-0.1566E-05
22.0	-0.1569E-05
23.0	-0.1571E-05
24.0	-0.1573E-05
25.0	-0.1574E-05
26.0	-0.1574E-05
27.0	-0.1575E-05
28.0	-0.1578E-05
29.0	-0.1578E-05
30.0	-0.1578E-05
30.7	-0.1578E-05

T=289.8DEG.K	
H (KOE)	E (OHM CM.)
0.0	0.0
1.0	-0.2518E-06
2.0	-0.4347E-06
3.0	-0.6131E-06
4.0	-0.7730E-06
5.0	-0.8978E-06
6.0	-0.9941E-06
8.0	-0.1145E-05
10.0	-0.1250E-05
13.0	-0.1366E-05
16.0	-0.1458E-05
20.0	-0.1553E-05
21.0	-0.1574E-05
22.0	-0.1594E-05
23.0	-0.1612E-05
24.0	-0.1627E-05
25.0	-0.1642E-05
26.0	-0.1657E-05
27.0	-0.1670E-05
28.0	-0.1682E-05
29.0	-0.1693E-05
30.0	-0.1704E-05
30.7	-0.1711E-05

T=320.2DEG.K	
H (KOE)	E (OHM CM.)
0.0	0.0
1.0	-0.5689E-07
2.0	-0.9627E-07
3.0	-0.1378E-06
4.0	-0.1783E-06
5.0	-0.2199E-06
6.0	-0.2593E-06
8.0	-0.3391E-06
10.0	-0.4135E-06
13.0	-0.5240E-06
16.0	-0.6301E-06
20.0	-0.7625E-06
21.0	-0.7932E-06
22.0	-0.8216E-06
23.0	-0.8489E-06
24.0	-0.8774E-06
25.0	-0.9036E-06
26.0	-0.9299E-06
27.0	-0.9583E-06
28.0	-0.9835E-06
29.0	-0.1008E-05
30.0	-0.1032E-05
30.7	-0.1050E-05

T=243.3DEG.K	
H (KOE)	E (OHM CM.)
0.0	0.0
1.0	-0.1422E-06
2.0	-0.2385E-06
3.0	-0.3359E-06
4.0	-0.4310E-06
5.0	-0.5339E-06
6.0	-0.6400E-06
8.0	-0.8391E-06
10.0	-0.1004E-05
13.0	-0.1187E-05
16.0	-0.1272E-05
20.0	-0.1308E-05
21.0	-0.1312E-05
22.0	-0.1313E-05
23.0	-0.1314E-05
24.0	-0.1316E-05
25.0	-0.1316E-05
26.0	-0.1316E-05
27.0	-0.1315E-05
28.0	-0.1316E-05
29.0	-0.1314E-05
30.0	-0.1312E-05
30.7	-0.1312E-05

T=280.5DEG.K	
H (KOE)	E (OHM CM.)
0.0	0.0
1.0	-0.2291E-06
2.0	-0.3780E-06
3.0	-0.5278E-06
4.0	-0.6835E-06
5.0	-0.8422E-06
6.0	-0.1000E-05
8.0	-0.1275E-05
10.0	-0.1405E-05
13.0	-0.1505E-05
16.0	-0.1567E-05
20.0	-0.1626E-05
21.0	-0.1637E-05
22.0	-0.1648E-05
23.0	-0.1656E-05
24.0	-0.1666E-05
25.0	-0.1674E-05
26.0	-0.1683E-05
27.0	-0.1690E-05
28.0	-0.1696E-05
29.0	-0.1703E-05
30.0	-0.1708E-05
30.7	-0.1713E-05

T=297.4DEG.K	
H (KOE)	E (OHM CM.)
0.0	0.0
1.0	-0.1880E-06
2.0	-0.3083E-06
3.0	-0.4198E-06
4.0	-0.5203E-06
5.0	-0.6154E-06
6.0	-0.7007E-06
8.0	-0.8483E-06
10.0	-0.9663E-06
13.0	-0.1110E-05
16.0	-0.1222E-05
20.0	-0.1339E-05
21.0	-0.1366E-05
22.0	-0.1388E-05
23.0	-0.1410E-05
24.0	-0.1431E-05
25.0	-0.1452E-05
26.0	-0.1471E-05
27.0	-0.1489E-05
28.0	-0.1506E-05
29.0	-0.1525E-05
30.0	-0.1539E-05
30.7	-0.1550E-05

T=339.7DEG.K	
H (KOE)	E (OHM CM.)
0.0	0.0
1.0	-0.3498E-07
2.0	-0.6121E-07
3.0	-0.8526E-07
4.0	-0.1093E-06
5.0	-0.1355E-06
6.0	-0.1585E-06
8.0	-0.2066E-06
10.0	-0.2558E-06
13.0	-0.3247E-06
16.0	-0.3968E-06
20.0	-0.4864E-06
21.0	-0.5116E-06
22.0	-0.5324E-06
23.0	-0.5531E-06
24.0	-0.5750E-06
25.0	-0.5947E-06
26.0	-0.6154E-06
27.0	-0.6362E-06
28.0	-0.6581E-06
29.0	-0.6799E-06
30.0	-0.6985E-06
30.7	-0.7139E-06

Figure 26. Experimental data for a gadolinium a-axis sample (Gd II)

T= 4.9DEG.K	
H (KOE)	E (OHM CM.)
0.0	0.0
1.0	-0.4689E-08
2.0	-0.9378E-08
3.0	-0.1485E-07
4.0	-0.1876E-07
5.0	-0.2266E-07
6.0	-0.2735E-07
8.0	-0.3595E-07
10.0	-0.4376E-07
13.0	-0.5627E-07
16.0	-0.6799E-07
20.0	-0.8753E-07
21.0	-0.9144E-07
22.0	-0.9691E-07
23.0	-0.1016E-06
24.0	-0.1086E-06
25.0	-0.1149E-06
26.0	-0.1211E-06
27.0	-0.1282E-06
28.0	-0.1329E-06
29.0	-0.1383E-06
30.0	-0.1422E-06
30.7	-0.1454E-06

T= 47.7DEG.K	
H (KOE)	E (OHM CM.)
0.0	0.0
1.0	-0.9363E-08
2.0	-0.1560E-07
3.0	-0.2029E-07
4.0	-0.2653E-07
5.0	-0.3355E-07
6.0	-0.3901E-07
8.0	-0.4838E-07
10.0	-0.6086E-07
13.0	-0.7412E-07
16.0	-0.8973E-07
20.0	-0.1108E-06
21.0	-0.1155E-06
22.0	-0.1194E-06
23.0	-0.1248E-06
24.0	-0.1311E-06
25.0	-0.1358E-06
26.0	-0.1389E-06
27.0	-0.1428E-06
28.0	-0.1459E-06
29.0	-0.1506E-06
30.0	-0.1537E-06
30.7	-0.1553E-06

T=121.6DEG.K	
H (KOE)	E (OHM CM.)
0.0	0.0
1.0	-0.2958E-07
2.0	-0.4670E-07
3.0	-0.6538E-07
4.0	-0.8173E-07
5.0	-0.9963E-07
6.0	-0.1160E-06
8.0	-0.1518E-06
10.0	-0.1876E-06
13.0	-0.2390E-06
16.0	-0.2849E-06
20.0	-0.3324E-06
21.0	-0.3417E-06
22.0	-0.3479E-06
23.0	-0.3534E-06
24.0	-0.3580E-06
25.0	-0.3635E-06
26.0	-0.3674E-06
27.0	-0.3713E-06
28.0	-0.3752E-06
29.0	-0.3798E-06
30.0	-0.3830E-06
30.7	-0.3861E-06

T=202.6DEG.K	
H (KOE)	E (OHM CM.)
0.0	0.0
1.0	-0.7628E-07
2.0	-0.1245E-06
3.0	-0.1736E-06
4.0	-0.2218E-06
5.0	-0.2732E-06
6.0	-0.3215E-06
8.0	-0.4226E-06
10.0	-0.5176E-06
13.0	-0.6484E-06
16.0	-0.7464E-06
20.0	-0.7791E-06
21.0	-0.7807E-06
22.0	-0.7807E-06
23.0	-0.7815E-06
24.0	-0.7815E-06
25.0	-0.7815E-06
26.0	-0.7807E-06
27.0	-0.7799E-06
28.0	-0.7807E-06
29.0	-0.7807E-06
30.0	-0.7807E-06
30.7	-0.7807E-06

T=245.3DEG.K	
H (KOE)	E (OHM CM.)
0.0	0.0
1.0	-0.1759E-06
2.0	-0.2885E-06
3.0	-0.4013E-06
4.0	-0.5117E-06
5.0	-0.6253E-06
6.0	-0.7334E-06
8.0	-0.9535E-06
10.0	-0.1154E-05
13.0	-0.1389E-05
16.0	-0.1459E-05
20.0	-0.1469E-05
21.0	-0.1470E-05
22.0	-0.1468E-05
23.0	-0.1468E-05
24.0	-0.1465E-05
25.0	-0.1464E-05
26.0	-0.1462E-05
27.0	-0.1461E-05
28.0	-0.1457E-05
29.0	-0.1455E-05
30.0	-0.1454E-05
30.7	-0.1452E-05

T= 21.5DEG.K	
H (KOE)	E (OHM CM.)
0.0	0.0
1.0	-0.6222E-08
2.0	-0.1089E-07
3.0	-0.1400E-07
4.0	-0.1867E-07
5.0	-0.2100E-07
6.0	-0.2567E-07
8.0	-0.3266E-07
10.0	-0.4278E-07
13.0	-0.5289E-07
16.0	-0.6611E-07
20.0	-0.8322E-07
21.0	-0.8711E-07
22.0	-0.9099E-07
23.0	-0.9566E-07
24.0	-0.1003E-06
25.0	-0.1042E-06
26.0	-0.1097E-06
27.0	-0.1135E-06
28.0	-0.1167E-06
29.0	-0.1198E-06
30.0	-0.1229E-06
30.7	-0.1252E-06

T= 78.4DEG.K	
H (KOE)	E (OHM CM.)
0.0	0.0
1.0	-0.1789E-07
2.0	-0.2878E-07
3.0	-0.4122E-07
4.0	-0.5289E-07
5.0	-0.6533E-07
6.0	-0.7700E-07
8.0	-0.1003E-06
10.0	-0.1221E-06
13.0	-0.1509E-06
16.0	-0.1765E-06
20.0	-0.2077E-06
21.0	-0.2147E-06
22.0	-0.2201E-06
23.0	-0.2263E-06
24.0	-0.2310E-06
25.0	-0.2364E-06
26.0	-0.2411E-06
27.0	-0.2458E-06
28.0	-0.2489E-06
29.0	-0.2535E-06
30.0	-0.2574E-06
30.7	-0.2613E-06

T=164.2DEG.K	
H (KOE)	E (OHM CM.)
0.0	0.0
1.0	-0.3979E-07
2.0	-0.6398E-07
3.0	-0.8973E-07
4.0	-0.1147E-06
5.0	-0.1404E-06
6.0	-0.1670E-06
8.0	-0.2200E-06
10.0	-0.2707E-06
13.0	-0.3425E-06
16.0	-0.4049E-06
20.0	-0.4572E-06
21.0	-0.4627E-06
22.0	-0.4666E-06
23.0	-0.4697E-06
24.0	-0.4736E-06
25.0	-0.4759E-06
26.0	-0.4783E-06
27.0	-0.4791E-06
28.0	-0.4814E-06
29.0	-0.4845E-06
30.0	-0.4945E-06
30.7	-0.4869E-06

T=229.0DEG.K	
H (KOE)	E (OHM CM.)
0.0	0.0
1.0	-0.1284E-06
2.0	-0.2117E-06
3.0	-0.2966E-06
4.0	-0.3791E-06
5.0	-0.4647E-06
6.0	-0.5456E-06
8.0	-0.7161E-06
10.0	-0.8780E-06
13.0	-0.1069E-05
16.0	-0.1165E-05
20.0	-0.1183E-05
21.0	-0.1182E-05
22.0	-0.1184E-05
23.0	-0.1182E-05
24.0	-0.1181E-05
25.0	-0.1180E-05
26.0	-0.1178E-05
27.0	-0.1176E-05
28.0	-0.1174E-05
29.0	-0.1173E-05
30.0	-0.1171E-05
30.7	-0.1169E-05

T=255.9DEG.K	
H (KOE)	E (OHM CM.)
0.0	0.0
1.0	-0.2050E-06
2.0	-0.3370E-06
3.0	-0.4659E-06
4.0	-0.5940E-06
5.0	-0.7237E-06
6.0	-0.8526E-06
8.0	-0.1109E-05
10.0	-0.1333E-05
13.0	-0.1556E-05
16.0	-0.1607E-05
20.0	-0.1621E-05
21.0	-0.1622E-05
22.0	-0.1621E-05
23.0	-0.1623E-05
24.0	-0.1623E-05
25.0	-0.1622E-05
26.0	-0.1623E-05
27.0	-0.1621E-05
28.0	-0.1620E-05
29.0	-0.1617E-05
30.0	-0.1617E-05
30.7	-0.1614E-05

Figure 27. Experimental data for a gadolinium a-axis sample (Gd III)

T=277.1DEG.K	
H (KOE)	E (OHM CM.)
0.0	0.0
1.0	-0.2704E-06
2.0	-0.4375E-06
3.0	-0.6077E-06
4.0	-0.7709E-06
5.0	-0.9403E-06
8.0	-0.1393E-05
10.0	-0.1581E-05
13.0	-0.1668E-05
16.0	-0.1712E-05
20.0	-0.1755E-05
21.0	-0.1762E-05
22.0	-0.1769E-05
23.0	-0.1774E-05
24.0	-0.1780E-05
25.0	-0.1785E-05
26.0	-0.1790E-05
27.0	-0.1794E-05
28.0	-0.1801E-05
29.0	-0.1804E-05
30.0	-0.1808E-05
30.7	-0.1810E-05

T=299.3DEG.K	
H (KOE)	E (OHM CM.)
0.0	0.0
1.0	-0.1355E-06
2.0	-0.2734E-06
3.0	-0.3762E-06
4.0	-0.4728E-06
5.0	-0.5679E-06
6.0	-0.6512E-06
8.0	-0.8062E-06
10.0	-0.9340E-06
13.0	-0.1091E-05
16.0	-0.1220E-05
20.0	-0.1358E-05
21.0	-0.1387E-05
22.0	-0.1415E-05
23.0	-0.1440E-05
24.0	-0.1464E-05
25.0	-0.1488E-05
26.0	-0.1511E-05
27.0	-0.1532E-05
28.0	-0.1550E-05
29.0	-0.1569E-05
30.0	-0.1587E-05
30.7	-0.1599E-05

T=319.5DEG.K	
H (KOE)	E (OHM CM.)
0.0	0.0
1.0	-0.6169E-07
2.0	-0.1054E-06
3.0	-0.1484E-06
4.0	-0.1898E-06
5.0	-0.2343E-06
6.0	-0.2757E-06
8.0	-0.3569E-06
10.0	-0.4373E-06
13.0	-0.5536E-06
16.0	-0.6614E-06
20.0	-0.8004E-06
21.0	-0.8324E-06
22.0	-0.8636E-06
23.0	-0.8933E-06
24.0	-0.9230E-06
25.0	-0.9519E-06
26.0	-0.9792E-06
27.0	-0.1007E-05
28.0	-0.1034E-05
29.0	-0.1060E-05
30.0	-0.1086E-05
30.7	-0.1105E-05

T=346.8DEG.K	
H (KOE)	E (OHM CM.)
0.0	0.0
1.0	-0.3194E-07
2.0	-0.5375E-07
3.0	-0.7478E-07
4.0	-0.9504E-07
5.0	-0.1192E-06
6.0	-0.1410E-06
8.0	-0.1862E-06
10.0	-0.2298E-06
13.0	-0.2937E-06
16.0	-0.3568E-06
20.0	-0.4409E-06
21.0	-0.4627E-06
22.0	-0.4830E-06
23.0	-0.5017E-06
24.0	-0.5219E-06
25.0	-0.5406E-06
26.0	-0.5616E-06
27.0	-0.5811E-06
28.0	-0.5998E-06
29.0	-0.6209E-06
30.0	-0.6411E-06
30.7	-0.6536E-06

T=293.4DEG.K	
H (KOE)	E (OHM CM.)
0.0	0.0
1.0	-0.2617E-06
2.0	-0.4230E-06
3.0	-0.5671E-06
4.0	-0.6925E-06
5.0	-0.8070E-06
6.0	-0.8997E-06
8.0	-0.1054E-05
10.0	-0.1172E-05
13.0	-0.1307E-05
16.0	-0.1411E-05
20.0	-0.1520E-05
21.0	-0.1544E-05
22.0	-0.1565E-05
23.0	-0.1584E-05
24.0	-0.1602E-05
25.0	-0.1621E-05
26.0	-0.1638E-05
27.0	-0.1655E-05
28.0	-0.1670E-05
29.0	-0.1685E-05
30.0	-0.1698E-05
30.7	-0.1709E-05

T=311.4DEG.K	
H (KOE)	E (OHM CM.)
0.0	0.0
1.0	-0.8471E-07
2.0	-0.1438E-06
3.0	-0.2005E-06
4.0	-0.2572E-06
5.0	-0.3140E-06
6.0	-0.3676E-06
8.0	-0.4771E-06
10.0	-0.5789E-06
13.0	-0.7173E-06
16.0	-0.8455E-06
20.0	-0.9939E-06
21.0	-0.1030E-05
22.0	-0.1062E-05
23.0	-0.1091E-05
24.0	-0.1122E-05
25.0	-0.1151E-05
26.0	-0.1179E-05
27.0	-0.1207E-05
28.0	-0.1234E-05
29.0	-0.1260E-05
30.0	-0.1285E-05
30.7	-0.1302E-05

T=329.8DEG.K	
H (KOE)	E (OHM CM.)
0.0	0.0
1.0	-0.4674E-07
2.0	-0.7946E-07
3.0	-0.1106E-06
4.0	-0.1418E-06
5.0	-0.1745E-06
6.0	-0.2057E-06
8.0	-0.2695E-06
10.0	-0.3295E-06
13.0	-0.4207E-06
16.0	-0.5087E-06
20.0	-0.6224E-06
21.0	-0.6497E-06
22.0	-0.6762E-06
23.0	-0.7011E-06
24.0	-0.7276E-06
25.0	-0.7525E-06
26.0	-0.7782E-06
27.0	-0.8024E-06
28.0	-0.8288E-06
29.0	-0.8530E-06
30.0	-0.8771E-06
30.7	-0.8935E-06

Figure 28. Experimental data for a gadolinium a-axis sample (Gd III)

T= 4.80EG.K	
H (KOE)	E (OHM CM.)
0.0	0.0
1.0	0.5522E-08
2.0	0.9940E-08
3.0	0.1104E-07
4.0	0.1657E-07
5.0	0.1657E-07
6.0	0.2098E-07
8.0	0.2651E-07
10.0	0.3424E-07
13.0	0.4086E-07
16.0	0.5633E-07
20.0	0.7068E-07
21.0	0.7841E-07
22.0	0.8173E-07
23.0	0.8614E-07
24.0	0.8946E-07
25.0	0.9608E-07
26.0	0.1005E-06
27.0	0.1038E-06
28.0	0.1082E-06
29.0	0.1138E-06
30.0	0.1193E-06
30.7	0.1226E-06

T= 31.1DEG.K	
H (KOE)	E (OHM CM.)
0.0	0.0
1.0	0.0
2.0	0.1110E-08
3.0	-0.1110E-08
4.0	0.0
5.0	0.1110E-08
6.0	0.2220E-08
8.0	0.2220E-08
10.0	0.0
13.0	-0.2220E-08
16.0	0.1110E-08
20.0	0.1665E-07
21.0	0.2220E-07
22.0	0.2663E-07
23.0	0.3107E-07
24.0	0.3440E-07
25.0	0.3995E-07
26.0	0.4550E-07
27.0	0.4883E-07
28.0	0.5327E-07
29.0	0.5882E-07
30.0	0.6437E-07
30.7	0.6659E-07

T= 60.1DEG.K	
H (KOE)	E (OHM CM.)
0.0	0.0
1.0	-0.3764E-07
2.0	-0.5978E-07
3.0	-0.8746E-07
4.0	-0.1140E-06
5.0	-0.1428E-06
6.0	-0.1705E-06
8.0	-0.2325E-06
10.0	-0.2912E-06
13.0	-0.3631E-06
16.0	-0.3930E-06
20.0	-0.3997E-06
21.0	-0.3986E-06
22.0	-0.3974E-06
23.0	-0.3952E-06
24.0	-0.3941E-06
25.0	-0.3897E-06
26.0	-0.3897E-06
27.0	-0.3897E-06
28.0	-0.3853E-06
29.0	-0.3808E-06
30.0	-0.3786E-06
30.7	-0.3764E-06

T= 77.6DEG.K	
H (KOE)	E (OHM CM.)
0.0	0.0
1.0	-0.7860E-07
2.0	-0.1340E-06
3.0	-0.1926E-06
4.0	-0.2502E-06
5.0	-0.3100E-06
6.0	-0.3676E-06
8.0	-0.4860E-06
10.0	-0.6034E-06
13.0	-0.7628E-06
16.0	-0.8702E-06
20.0	-0.9045E-06
21.0	-0.9045E-06
22.0	-0.9012E-06
23.0	-0.9001E-06
24.0	-0.8967E-06
25.0	-0.8956E-06
26.0	-0.8912E-06
27.0	-0.8890E-06
28.0	-0.8868E-06
29.0	-0.8835E-06
30.0	-0.8801E-06
30.7	-0.8790E-06

T= 94.0DEG.K	
H (KOE)	E (OHM CM.)
0.0	0.0
1.0	-0.1416E-06
2.0	-0.2411E-06
3.0	-0.3440E-06
4.0	-0.4425E-06
5.0	-0.5454E-06
6.0	-0.6449E-06
8.0	-0.8485E-06
10.0	-0.1048E-05
13.0	-0.1306E-05
16.0	-0.1436E-05
20.0	-0.1503E-05
21.0	-0.1509E-05
22.0	-0.1511E-05
23.0	-0.1510E-05
24.0	-0.1508E-05
25.0	-0.1506E-05
26.0	-0.1503E-05
27.0	-0.1501E-05
28.0	-0.1498E-05
29.0	-0.1496E-05
30.0	-0.1492E-05
30.7	-0.1490E-05

T= 20.1DEG.K	
H (KOE)	E (OHM CM.)
0.0	0.0
1.0	0.6648E-08
2.0	0.9972E-08
3.0	0.1330E-07
4.0	0.1662E-07
5.0	0.1884E-07
6.0	0.2105E-07
8.0	0.2548E-07
10.0	0.3213E-07
13.0	0.3989E-07
16.0	0.5429E-07
20.0	0.7202E-07
21.0	0.7645E-07
22.0	0.8199E-07
23.0	0.8864E-07
24.0	0.9085E-07
25.0	0.9529E-07
26.0	0.9972E-07
27.0	0.1064E-06
28.0	0.1119E-06
29.0	0.1163E-06
30.0	0.1219E-06
30.7	0.1252E-06

T= 47.0DEG.K	
H (KOE)	E (OHM CM.)
0.0	0.0
1.0	-0.1436E-07
2.0	-0.2098E-07
3.0	-0.3313E-07
4.0	-0.4197E-07
5.0	-0.5301E-07
6.0	-0.6516E-07
8.0	-0.8946E-07
10.0	-0.1127E-06
13.0	-0.1403E-06
16.0	-0.1524E-06
20.0	-0.1458E-06
21.0	-0.1436E-06
22.0	-0.1403E-06
23.0	-0.1381E-06
24.0	-0.1347E-06
25.0	-0.1292E-06
26.0	-0.1259E-06
27.0	-0.1237E-06
28.0	-0.1204E-06
29.0	-0.1182E-06
30.0	-0.1171E-06
30.7	-0.1127E-06

T= 68.5DEG.K	
H (KOE)	E (OHM CM.)
0.0	0.0
1.0	-0.5403E-07
2.0	-0.8711E-07
3.0	-0.1312E-06
4.0	-0.1742E-06
5.0	-0.2205E-06
6.0	-0.2646E-06
8.0	-0.3584E-06
10.0	-0.4488E-06
13.0	-0.5436E-06
16.0	-0.5855E-06
20.0	-0.6031E-06
21.0	-0.6054E-06
22.0	-0.6054E-06
23.0	-0.6065E-06
24.0	-0.6054E-06
25.0	-0.6054E-06
26.0	-0.6020E-06
27.0	-0.5998E-06
28.0	-0.5954E-06
29.0	-0.5921E-06
30.0	-0.5899E-06
30.7	-0.5877E-06

T= 86.0DEG.K	
H (KOE)	E (OHM CM.)
0.0	0.0
1.0	-0.1169E-06
2.0	-0.1919E-06
3.0	-0.2768E-06
4.0	-0.3617E-06
5.0	-0.4510E-06
6.0	-0.5414E-06
8.0	-0.7244E-06
10.0	-0.8832E-06
13.0	-0.1030E-05
16.0	-0.1109E-05
20.0	-0.1164E-05
21.0	-0.1170E-05
22.0	-0.1174E-05
23.0	-0.1177E-05
24.0	-0.1177E-05
25.0	-0.1179E-05
26.0	-0.1179E-05
27.0	-0.1177E-05
28.0	-0.1174E-05
29.0	-0.1171E-05
30.0	-0.1170E-05
30.7	-0.1168E-05

T=113.1DEG.K	
H (KOE)	E (OHM CM.)
0.0	0.0
1.0	-0.2393E-06
2.0	-0.4025E-06
3.0	-0.5767E-06
4.0	-0.7597E-06
5.0	-0.9527E-06
6.0	-0.1134E-05
8.0	-0.1458E-05
10.0	-0.1667E-05
13.0	-0.1903E-05
16.0	-0.2064E-05
20.0	-0.2188E-05
21.0	-0.2207E-05
22.0	-0.2221E-05
23.0	-0.2232E-05
24.0	-0.2239E-05
25.0	-0.2243E-05
26.0	-0.2247E-05
27.0	-0.2251E-05
28.0	-0.2249E-05
29.0	-0.2252E-05
30.0	-0.2251E-05
30.7	-0.2249E-05

Figure 29. Experimental data for the gadolinium c-axis sample (Gd IV)

T=125.9DEG.K	
H (KOE)	E (OHM CM.)
0.0	0.0
1.0	-0.3077E-06
2.0	-0.5187E-06
3.0	-0.7441E-06
4.0	-0.9763E-06
5.0	-0.1220E-05
6.0	-0.1445E-05
8.0	-0.1827E-05
10.0	-0.2090E-05
13.0	-0.2383E-05
16.0	-0.2592E-05
20.0	-0.2761E-05
21.0	-0.2789E-05
22.0	-0.2803E-05
23.0	-0.2818E-05
24.0	-0.2828E-05
25.0	-0.2837E-05
26.0	-0.2841E-05
27.0	-0.2847E-05
28.0	-0.2849E-05
29.0	-0.2852E-05
30.0	-0.2853E-05
30.7	-0.2852E-05

T=155.4DEG.K	
H (KOE)	E (OHM CM.)
0.0	0.0
1.0	-0.4945E-06
2.0	-0.8396E-06
3.0	-0.1191E-05
4.0	-0.1533E-05
5.0	-0.1874E-05
6.0	-0.2173E-05
8.0	-0.2696E-05
10.0	-0.3112E-05
13.0	-0.3602E-05
16.0	-0.3954E-05
20.0	-0.4213E-05
21.0	-0.4249E-05
22.0	-0.4273E-05
23.0	-0.4291E-05
24.0	-0.4303E-05
25.0	-0.4313E-05
26.0	-0.4321E-05
27.0	-0.4327E-05
28.0	-0.4332E-05
29.0	-0.4334E-05
30.0	-0.4335E-05
30.7	-0.4337E-05

T=166.2DEG.K	
H (KOE)	E (OHM CM.)
0.0	0.0
1.0	-0.5288E-06
2.0	-0.9060E-06
3.0	-0.1288E-05
4.0	-0.1660E-05
5.0	-0.2043E-05
6.0	-0.2412E-05
8.0	-0.3081E-05
10.0	-0.3610E-05
13.0	-0.4253E-05
16.0	-0.4698E-05
20.0	-0.4916E-05
21.0	-0.4930E-05
22.0	-0.4940E-05
23.0	-0.4946E-05
24.0	-0.4951E-05
25.0	-0.4954E-05
26.0	-0.4956E-05
27.0	-0.4956E-05
28.0	-0.4956E-05
29.0	-0.4956E-05
30.0	-0.4956E-05
30.7	-0.4955E-05

T=206.0DEG.K	
H (KOE)	E (OHM CM.)
0.0	0.0
1.0	-0.7019E-06
2.0	-0.1207E-05
3.0	-0.1714E-05
4.0	-0.2216E-05
5.0	-0.2730E-05
6.0	-0.3219E-05
8.0	-0.4185E-05
10.0	-0.5023E-05
13.0	-0.5997E-05
16.0	-0.6500E-05
20.0	-0.6649E-05
21.0	-0.6667E-05
22.0	-0.6679E-05
23.0	-0.6689E-05
24.0	-0.6698E-05
25.0	-0.6705E-05
26.0	-0.6713E-05
27.0	-0.6719E-05
28.0	-0.6721E-05
29.0	-0.6727E-05
30.0	-0.6730E-05
30.7	-0.6733E-05

T=232.8DEG.K	
H (KOE)	E (OHM CM.)
0.0	0.0
1.0	-0.8248E-06
2.0	-0.1378E-05
3.0	-0.1944E-05
4.0	-0.2504E-05
5.0	-0.3071E-05
6.0	-0.3596E-05
8.0	-0.4578E-05
10.0	-0.5415E-05
13.0	-0.6319E-05
16.0	-0.6762E-05
20.0	-0.6979E-05
21.0	-0.7009E-05
22.0	-0.7033E-05
23.0	-0.7055E-05
24.0	-0.7074E-05
25.0	-0.7093E-05
26.0	-0.7110E-05
27.0	-0.7124E-05
28.0	-0.7138E-05
29.0	-0.7152E-05
30.0	-0.7165E-05
30.7	-0.7173E-05

T=136.4DEG.K	
H (KOE)	E (OHM CM.)
0.0	0.0
1.0	-0.3667E-06
2.0	-0.6238E-06
3.0	-0.8820E-06
4.0	-0.1139E-05
5.0	-0.1402E-05
6.0	-0.1658E-05
8.0	-0.2169E-05
10.0	-0.2556E-05
13.0	-0.2958E-05
16.0	-0.3239E-05
20.0	-0.3414E-05
21.0	-0.3428E-05
22.0	-0.3436E-05
23.0	-0.3438E-05
24.0	-0.3441E-05
25.0	-0.3442E-05
26.0	-0.3444E-05
27.0	-0.3441E-05
28.0	-0.3441E-05
29.0	-0.3440E-05
30.0	-0.3439E-05
30.7	-0.3440E-05

T=158.8DEG.K	
H (KOE)	E (OHM CM.)
0.0	0.0
1.0	-0.5165E-06
2.0	-0.8719E-06
3.0	-0.1234E-05
4.0	-0.1587E-05
5.0	-0.1938E-05
6.0	-0.2245E-05
8.0	-0.2789E-05
10.0	-0.3223E-05
13.0	-0.3740E-05
16.0	-0.4111E-05
20.0	-0.4384E-05
21.0	-0.4424E-05
22.0	-0.4447E-05
23.0	-0.4466E-05
24.0	-0.4479E-05
25.0	-0.4489E-05
26.0	-0.4497E-05
27.0	-0.4502E-05
28.0	-0.4506E-05
29.0	-0.4509E-05
30.0	-0.4509E-05
30.7	-0.4513E-05

T=193.8DEG.K	
H (KOE)	E (OHM CM.)
0.0	0.0
1.0	-0.6997E-06
2.0	-0.1185E-05
3.0	-0.1668E-05
4.0	-0.2127E-05
5.0	-0.2574E-05
6.0	-0.2985E-05
8.0	-0.3756E-05
10.0	-0.4416E-05
13.0	-0.5208E-05
16.0	-0.5735E-05
20.0	-0.6054E-05
21.0	-0.6090E-05
22.0	-0.6117E-05
23.0	-0.6139E-05
24.0	-0.6158E-05
25.0	-0.6168E-05
26.0	-0.6179E-05
27.0	-0.6189E-05
28.0	-0.6196E-05
29.0	-0.6203E-05
30.0	-0.6207E-05
30.7	-0.6212E-05

T=224.1DEG.K	
H (KOE)	E (OHM CM.)
0.0	0.0
1.0	-0.7863E-06
3.0	-0.1870E-05
4.0	-0.2412E-05
5.0	-0.2953E-05
6.0	-0.3451E-05
8.0	-0.4399E-05
10.0	-0.5214E-05
13.0	-0.6139E-05
16.0	-0.6652E-05
20.0	-0.6905E-05
21.0	-0.6939E-05
22.0	-0.6964E-05
23.0	-0.6985E-05
24.0	-0.7006E-05
25.0	-0.7022E-05
26.0	-0.7037E-05
27.0	-0.7049E-05
28.0	-0.7062E-05
29.0	-0.7074E-05
30.0	-0.7085E-05
30.7	-0.7091E-05

T=243.5DEG.K	
H (KOE)	E (OHM CM.)
0.0	0.0
1.0	-0.8002E-06
2.0	-0.1386E-05
3.0	-0.1978E-05
4.0	-0.2564E-05
5.0	-0.3162E-05
6.0	-0.3729E-05
8.0	-0.4862E-05
10.0	-0.5852E-05
13.0	-0.6690E-05
16.0	-0.6912E-05
20.0	-0.7041E-05
21.0	-0.7066E-05
22.0	-0.7088E-05
23.0	-0.7109E-05
24.0	-0.7129E-05
25.0	-0.7146E-05
26.0	-0.7163E-05
27.0	-0.7182E-05
28.0	-0.7199E-05
29.0	-0.7215E-05
30.0	-0.7230E-05
30.7	-0.7240E-05

Figure 30. Experimental data for the gadolinium c-axis sample (Gd IV)

T=255.9DEG.K	
H (KOE)	E (OHM CM.)
0.0	0.0
1.0	-0.8790E-06
2.0	-0.1459E-05
3.0	-0.2043E-05
4.0	-0.2620E-05
5.0	-0.3204E-05
6.0	-0.3740E-05
8.0	-0.4711E-05
10.0	-0.5451E-05
13.0	-0.6085E-05
16.0	-0.6359E-05
20.0	-0.6552E-05
21.0	-0.6590E-05
22.0	-0.6621E-05
23.0	-0.6651E-05
24.0	-0.6680E-05
25.0	-0.6708E-05
26.0	-0.6736E-05
27.0	-0.6761E-05
28.0	-0.6788E-05
29.0	-0.6811E-05
30.0	-0.6834E-05
30.7	-0.6850E-05

T=273.9DEG.K	
H (KOE)	E (OHM CM.)
0.0	0.0
1.0	-0.8046E-06
2.0	-0.1395E-05
3.0	-0.1989E-05
4.0	-0.2568E-05
5.0	-0.3155E-05
6.0	-0.3697E-05
8.0	-0.4639E-05
10.0	-0.5041E-05
13.0	-0.5286E-05
16.0	-0.5372E-05
20.0	-0.5466E-05
21.0	-0.5490E-05
22.0	-0.5512E-05
23.0	-0.5530E-05
24.0	-0.5550E-05
25.0	-0.5568E-05
26.0	-0.5584E-05
27.0	-0.5602E-05
28.0	-0.5620E-05
29.0	-0.5638E-05
30.0	-0.5653E-05
30.7	-0.5663E-05

T=286.0DEG.K	
H (KOE)	E (OHM CM.)
0.0	0.0
1.0	-0.7680E-06
2.0	-0.1335E-05
3.0	-0.1887E-05
4.0	-0.2414E-05
5.0	-0.2899E-05
6.0	-0.3244E-05
8.0	-0.3595E-05
10.0	-0.3844E-05
13.0	-0.4142E-05
16.0	-0.4389E-05
20.0	-0.4669E-05
21.0	-0.4735E-05
22.0	-0.4794E-05
23.0	-0.4849E-05
24.0	-0.4905E-05
25.0	-0.4958E-05
26.0	-0.5012E-05
27.0	-0.5064E-05
28.0	-0.5115E-05
29.0	-0.5164E-05
30.0	-0.5209E-05
30.7	-0.5243E-05

T=299.8DEG.K	
H (KOE)	E (OHM CM.)
0.0	0.0
1.0	-0.3432E-06
2.0	-0.6045E-06
3.0	-0.8536E-06
4.0	-0.1088E-05
5.0	-0.1310E-05
6.0	-0.1510E-05
8.0	-0.1766E-05
10.0	-0.2185E-05
13.0	-0.2578E-05
16.0	-0.2912E-05
20.0	-0.3284E-05
21.0	-0.3373E-05
22.0	-0.3455E-05
23.0	-0.3530E-05
24.0	-0.3606E-05
25.0	-0.3677E-05
26.0	-0.3749E-05
27.0	-0.3817E-05
28.0	-0.3885E-05
29.0	-0.3948E-05
30.0	-0.4013E-05
30.7	-0.4054E-05

T=322.2DEG.K	
H (KOE)	E (OHM CM.)
0.0	0.0
1.0	-0.1133E-06
2.0	-0.1988E-06
3.0	-0.2821E-06
4.0	-0.3687E-06
5.0	-0.4554E-06
6.0	-0.5398E-06
8.0	-0.7108E-06
10.0	-0.8774E-06
13.0	-0.1116E-05
16.0	-0.1353E-05
20.0	-0.1650E-05
21.0	-0.1726E-05
22.0	-0.1795E-05
23.0	-0.1865E-05
24.0	-0.1935E-05
25.0	-0.2000E-05
26.0	-0.2067E-05
27.0	-0.2135E-05
28.0	-0.2199E-05
29.0	-0.2264E-05
30.0	-0.2328E-05
30.7	-0.2373E-05

T=268.8DEG.K	
H (KOE)	E (OHM CM.)
0.0	0.0
1.0	-0.8541E-06
2.0	-0.1432E-05
3.0	-0.2015E-05
4.0	-0.2589E-05
5.0	-0.3169E-05
8.0	-0.4599E-05
10.0	-0.5143E-05
13.0	-0.5527E-05
16.0	-0.5733E-05
20.0	-0.5930E-05
21.0	-0.5974E-05
22.0	-0.6012E-05
23.0	-0.6051E-05
24.0	-0.6088E-05
25.0	-0.6122E-05
26.0	-0.6159E-05
27.0	-0.6192E-05
28.0	-0.6225E-05
29.0	-0.6257E-05
30.0	-0.6291E-05
30.7	-0.6311E-05

T=281.9DEG.K	
H (KOE)	E (OHM CM.)
0.0	0.0
1.0	-0.8365E-06
2.0	-0.1397E-05
3.0	-0.1958E-05
4.0	-0.2500E-05
5.0	-0.3021E-05
6.0	-0.3438E-05
8.0	-0.3939E-05
10.0	-0.4216E-05
13.0	-0.4502E-05
16.0	-0.4730E-05
20.0	-0.4980E-05
21.0	-0.5039E-05
22.0	-0.5091E-05
23.0	-0.5140E-05
24.0	-0.5191E-05
25.0	-0.5236E-05
26.0	-0.5285E-05
27.0	-0.5332E-05
28.0	-0.5376E-05
29.0	-0.5420E-05
30.0	-0.5461E-05
30.7	-0.5492E-05

T=292.8DEG.K	
H (KOE)	E (OHM CM.)
0.0	0.0
1.0	-0.7080E-06
2.0	-0.1160E-05
3.0	-0.1537E-05
4.0	-0.1854E-05
5.0	-0.2125E-05
6.0	-0.2346E-05
8.0	-0.2721E-05
10.0	-0.3019E-05
13.0	-0.3376E-05
16.0	-0.3672E-05
20.0	-0.4003E-05
21.0	-0.4081E-05
22.0	-0.4149E-05
23.0	-0.4218E-05
24.0	-0.4283E-05
25.0	-0.4346E-05
26.0	-0.4408E-05
27.0	-0.4468E-05
28.0	-0.4525E-05
29.0	-0.4583E-05
30.0	-0.4640E-05
30.7	-0.4678E-05

T=313.5DEG.K	
H (KOE)	E (OHM CM.)
0.0	0.0
1.0	-0.1512E-06
2.0	-0.2690E-06
3.0	-0.3879E-06
4.0	-0.5058E-06
5.0	-0.6269E-06
6.0	-0.7392E-06
8.0	-0.9693E-06
10.0	-0.1185E-05
13.0	-0.1493E-05
16.0	-0.1782E-05
20.0	-0.2133E-05
21.0	-0.2222E-05
22.0	-0.2302E-05
23.0	-0.2379E-05
24.0	-0.2454E-05
25.0	-0.2529E-05
26.0	-0.2602E-05
27.0	-0.2676E-05
28.0	-0.2746E-05
29.0	-0.2816E-05
30.0	-0.2884E-05
30.7	-0.2931E-05

T=331.8DEG.K	
H (KOE)	E (OHM CM.)
0.0	0.0
1.0	-0.8552E-07
2.0	-0.1488E-06
3.0	-0.2132E-06
4.0	-0.2766E-06
5.0	-0.3432E-06
6.0	-0.4065E-06
8.0	-0.5364E-06
10.0	-0.6642E-06
13.0	-0.8497E-06
16.0	-0.1038E-05
20.0	-0.1281E-05
21.0	-0.1343E-05
22.0	-0.1402E-05
23.0	-0.1459E-05
24.0	-0.1516E-05
25.0	-0.1569E-05
26.0	-0.1627E-05
27.0	-0.1686E-05
28.0	-0.1743E-05
29.0	-0.1799E-05
30.0	-0.1855E-05
30.7	-0.1895E-05

Figure 31. Experimental data for the gadolinium c-axis sample (Gd IV)